

Modelling light-cone distribution amplitudes from non-relativistic bound states

G. BELL^a AND TH. FELDMANN^{b,1}

^a *Institut für Theoretische Teilchenphysik,
Universität Karlsruhe, D-76128 Karlsruhe, Germany*

^b *Fachbereich Physik, Theoretische Physik I,
Universität Siegen, Emmy Noether Campus, D-57068 Siegen, Germany*

Abstract

We calculate light-cone distribution amplitudes for non-relativistic bound states, including radiative corrections from relativistic gluon exchange to first order in the strong coupling constant. We distinguish between bound states of quarks with equal (or similar) mass, $m_1 \sim m_2$, and between bound states where the quark masses are hierarchical, $m_1 \gg m_2$. For both cases we calculate the distribution amplitudes at the non-relativistic scale and discuss the renormalization-group evolution for the leading-twist and 2-particle distributions. Our results apply to hard exclusive reactions with non-relativistic bound states in the QCD factorization approach like, for instance, $B_c \rightarrow \eta_c \ell \nu$ or $e^+ e^- \rightarrow J/\psi \eta_c$. They also serve as a toy model for light-cone distribution amplitudes of light mesons or heavy B and D mesons, for which certain model-independent properties can be derived. In particular, we calculate the anomalous dimension for the B meson distribution amplitude $\phi_B^-(\omega)$ in the Wandzura-Wilczek approximation and derive the according solution of the evolution equation at leading logarithmic accuracy.

¹Also at: Technische Universität München, Physik Department, 85747 Garching, Germany.

Contents

1	Introduction	1
2	Light-cone distribution amplitudes and the non-relativistic limit	1
2.1	Non-relativistic approximation	1
2.2	Definition of LCDAs for light pseudoscalar mesons	2
2.2.1	Equations of motion	3
2.2.2	Tree-level result	3
2.3	Definition of LCDAs for heavy pseudoscalar mesons	4
2.3.1	Equations of motion	4
2.3.2	Tree-level result	5
3	Relativistic corrections at one-loop	6
3.1	Light mesons	6
3.1.1	Local matrix elements	6
3.1.2	The twist-2 LCDA $\phi_\pi(u)$	6
3.1.3	2-particle LCDAs of twist-3	9
3.2	Heavy mesons	9
3.2.1	The LCDA $\phi_B^+(\omega)$	9
3.2.2	The LCDA $\phi_B^-(\omega)$	11
3.2.3	3-particle LCDAs and equations of motion	12
4	Renormalization-group evolution	13
4.1	The twist-2 LCDA $\phi_\pi(u)$	13
4.2	The LCDA $\phi_B^+(\omega)$	15
4.3	The LCDA $\phi_B^-(\omega)$	18
5	Summary	20
A	One-loop corrections to $\phi_\pi(u)$	20
A.1	Vertex diagram	20
A.2	Wilson-line diagrams	21
B	One-loop corrections to $\phi_B^\pm(\omega)$	21
B.1	Vertex diagram	21
B.2	Wilson-line coupling to heavy quark	22
B.3	Wilson-line coupling to light quark	23
C	Equations of motion for heavy meson LCDAs	23
D	Solution of RGE for $\phi_B^-(\omega)$ in WW approximation	24

1 Introduction

Exclusive hadron reactions with large momentum transfer involve strong interaction dynamics at very different momentum scales. In cases where the hard-scattering process is dominated by light-like distances, the long-distance hadronic information is given in terms of so-called light-cone distribution amplitudes (LCDAs) which are defined from hadron-to-vacuum matrix elements of non-local operators with quark and gluon field operators separated along the light-cone [1, 2] and [3, 4]. LCDAs appear in the so-called pQCD approach to hard exclusive reactions [5–7], in the QCD factorization approach to heavy-to-light transitions [8], in soft-collinear effective theory [9, 10], as well as in the light-cone sum rule approach to exclusive decay amplitudes [11–13] (for a recent review, see [14]).

Representing universal hadronic properties, LCDAs can either be extracted from experimental data, or they have to be constrained by non-perturbative methods. The most extensively studied and probably best understood case is the leading-twist pion LCDA, for which phenomenological constraints [15–17] from the $\pi - \gamma$ transition form factor [18], as well as estimates for the lowest moments from QCD sum rules [2, 19, 20] and lattice QCD [21, 22] exist. On the other hand, our knowledge on LCDAs for heavy B mesons [3, 23, 24], and even more so for heavy quarkonia [25, 26], had been relatively poor until recently.

Although LCDAs, in general, are not calculable in QCD perturbation theory, their evolution with the factorization scale (which is set by the momentum transfer of the hard process) can be calculated and is well understood, both, for light mesons [5] and for heavy mesons [23]. The situation becomes somewhat simpler, if the hadron under consideration can be approximated as a non-relativistic bound state of two sufficiently heavy quarks. In this case we expect exclusive matrix elements – like transition form factors [27] and, in particular, the LCDAs – to be calculable perturbatively, since the quark masses provide an intrinsic physical infrared regulator.

In this article, we are going to calculate the LCDAs for non-relativistic meson bound states including relativistic QCD corrections to first order in the strong coupling constant at the non-relativistic matching scale which is set by the mass of the lighter quark in the hadron. We discuss twist-2 and twist-3 LCDAs for 2-particle Fock states with approximately equal quark masses (for instance an η_c meson), as well as 2-particle and 3-particle LCDAs for heavy mesons (like the B_c), where one of the quark masses is considered to be much larger than the second one ($m_b \gg m_c$). Our results can also be viewed as a toy model for possible parameterizations of LCDAs for relativistic bound states, like the pion, kaon or B_q meson at a low input scale, which may be evolved to the appropriate higher scales using the standard renormalization group equations in QCD (or HQET, respectively).

Our paper is organized as follows. In the following section we give a short introduction to the non-relativistic approximation and collect the definitions and properties of LCDAs for light and heavy mesons. The main result of our paper, the corrections from relativistic gluon exchange, are presented in Section 3. Here we also derive model-independent results for the B meson LCDAs ϕ_B^+ and ϕ_B^- , namely the cut-off dependence of positive moments and the anomalous dimension kernels, and investigate the impact of the 3-particle LCDAs to the Wandzura-Wilczek approximation beyond tree-level. We discuss the effect of QCD evolution above the non-relativistic matching scale in Section 4, including a new result for the B meson LCDA ϕ_B^- , before we conclude. Some technical details of the calculation are collected in an appendix. Some of our results have already appeared in a proceedings article [28].

2 Light-cone distribution amplitudes and the non-relativistic limit

2.1 Non-relativistic approximation

The wave function for a non-relativistic (NR) bound state of a quark and an antiquark with respective masses m_1 and m_2 can be obtained from the resummation of NR (*potential*) gluon exchange as

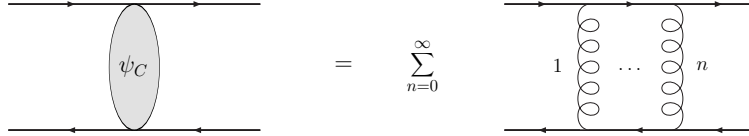


Figure 1: Resummation of potential gluons into a non-relativistic Coulomb wave-function.

sketched in Figure 1. The solution of the corresponding Schrödinger equation with Coulomb potential yields

$$\psi_C(\vec{p}) \propto \frac{\kappa^{5/2}}{(\kappa^2 + |\vec{p}|^2)^2}, \quad (1)$$

where $\kappa = m_r \alpha_s C_F$ and $m_r = m_1 m_2 / (m_1 + m_2)$ is the reduced mass. The normalization of the wave function gives the (non-relativistic) meson decay constant

$$f_{\text{NR}} = \frac{2\sqrt{N_c}}{\pi} \frac{\kappa^{3/2}}{(m_1 + m_2)^{1/2}}. \quad (2)$$

For more details and references to the original literature, see e.g. [29] (also [27]).

In this approximation, the \bar{B}_c meson is entirely dominated by the 2-particle Fock state built from a bottom quark with mass $m_1 \equiv M = m_b$ and a charm antiquark with mass $m_2 \equiv m = m_c$. Consequently to first approximation in the NR expansion, the \bar{B}_c meson consists of a quark with momentum Mv_μ and an antiquark with momentum mv_μ , where v_μ is the four-velocity of the \bar{B}_c meson ($v^2 = 1$). The spinor degrees of freedom for the \bar{B}_c meson are represented by the Dirac projector $\frac{1}{2}(1 + \not{v})\gamma_5$. Similarly, a pseudoscalar η_c meson is interpreted as a $c\bar{c}$ bound state where both constituents have approximately equal momenta mv_μ .

The non-relativistic approximation can also serve as a toy model for bound states of light (relativistic) quarks. We will in the following refer to “heavy mesons” as “ B ” (where we mean the realistic example of a B_c meson, or the toy model for a B_q meson) and “light mesons” as “ π ” (where the realistic example is η_c , and the toy-model application would be the pion or also the kaon for $m_1 \neq m_2$).

2.2 Definition of LCDAs for light pseudoscalar mesons

Following [1, 2] we define the 2-particle LCDAs of a light pseudoscalar meson via

$$\begin{aligned} \langle \pi(P) | \bar{q}_1(y) [y, x] \gamma_\mu \gamma_5 q_2(x) | 0 \rangle &= -i f_\pi \int_0^1 du e^{i(u p \cdot y + \bar{u} p \cdot x)} \left[p_\mu \phi_\pi(u) + \frac{m_\pi^2}{2 p \cdot z} z_\mu g_\pi(u) \right], \\ \langle \pi(P) | \bar{q}_1(y) [y, x] i \gamma_5 q_2(x) | 0 \rangle &= f_\pi \mu_\pi \int_0^1 du e^{i(u p \cdot y + \bar{u} p \cdot x)} \phi_p(u), \\ \langle \pi(P) | \bar{q}_1(y) [y, x] \sigma_{\mu\nu} \gamma_5 q_2(x) | 0 \rangle &= i f_\pi \tilde{\mu}_\pi (p_\mu z_\nu - p_\nu z_\mu) \int_0^1 du e^{i(u p \cdot y + \bar{u} p \cdot x)} \frac{\phi_\sigma(u)}{2D - 2} \end{aligned} \quad (3)$$

with two light-like vectors $z_\mu = y_\mu - x_\mu$ and $p_\mu = P_\mu - m_\pi^2 / (2P \cdot z) z_\mu$, and $u = 1 - \bar{u}$ denoting the light-cone momentum fraction of the quark q_1 . The gauge link factor is denoted as

$$[y, x] = \mathcal{P} \exp \left[i g_s \int_0^1 dt (y - x) \cdot A(ty + (1 - t)x) \right]. \quad (4)$$

$\phi_\pi(u)$ is the twist-2 LCDA, while $\phi_p(u)$ and $\phi_\sigma(u)$ are twist-3. For completeness, we have also quoted the twist-4 LCDA $g_\pi(u)$ which, like the 3-particle LCDAs, will not be considered further in

this work.² All LCDAs are normalized to 1, such that the prefactors in (3) are defined in the local limit $x \rightarrow y$. In the definition of $\phi_\sigma(u)$, we have included a factor $3/(D-1)$, such that the relation between μ_π and $\tilde{\mu}_\pi$ from the equations of motion (see below) is maintained in $D \neq 4$ dimensions.

2.2.1 Equations of motion

The equations of motion (eom) provide relations between the matrix elements defined in (3). Following [2] we obtain

$$\begin{aligned} \frac{m_\pi^2}{2} [\phi_\pi(u) + g_\pi(u)] &= (m_1 + m_2) \mu_\pi \phi_p(u) + \dots, \\ \mu_\pi \phi_p(u) + \frac{\tilde{\mu}_\pi}{D-1} \left[(2-D) \phi_\sigma(u) + \frac{2u-1}{2} \phi'_\sigma(u) \right] &= (m_1 + m_2) \phi_\pi(u) + \dots, \\ (2u-1) \mu_\pi \phi_p(u) + \frac{\tilde{\mu}_\pi}{2D-2} \phi'_\sigma(u) &= (m_1 - m_2) \phi_\pi(u) + \dots, \end{aligned} \quad (5)$$

where the ellipsis denote contributions from 3-particle LCDAs which we do not specify here. In the local limit the contributions from the 3-particle LCDAs drop out and integration of (5) yields

$$\mu_\pi = \frac{m_\pi^2}{m_1 + m_2}, \quad \tilde{\mu}_\pi = \mu_\pi - (m_1 + m_2) \quad (6)$$

and

$$\int_0^1 du u \phi_p(u) = \frac{1}{2} + \frac{m_1 - m_2}{2\mu_\pi}. \quad (7)$$

Notice that the relations (5,6,7) hold for the *bare* (unrenormalized) parameters and distribution amplitudes.

2.2.2 Tree-level result

At tree level, and in leading order of the expansion in the relative velocities, the quark and the antiquark in the NR wave function simply share the momentum of the meson according to their masses, $p_i^\mu \simeq m_i/(m_1 + m_2)P^\mu$. For "light" mesons this implies³

$$\phi_\pi(u) \simeq \phi_p(u) \simeq g_\pi(u) \simeq \delta(u - u_0), \quad (8)$$

with $u_0 = m_1/(m_1 + m_2)$ and $\bar{u}_0 = m_2/(m_1 + m_2)$. Consequently, all positive and negative moments of the distribution amplitudes are simply given in terms of the corresponding power of u_0 . Often, one is interested in the coefficients a_n of an expansion of $\phi_\pi(u; \mu)$ in terms of Gegenbauer polynomials,

$$\phi_\pi(u; \mu) = 6u\bar{u} \left(1 + \sum_{n=1}^{\infty} a_n(\mu) C_n^{3/2}(2u-1) \right), \quad (9)$$

which are the eigenfunctions of the LO evolution kernel, see Section 4.1 below. For the particular form in (8), the Gegenbauer coefficients are given by

$$a_n = \frac{2(2n+3)}{3(2+n)(1+n)} \int_0^1 du \phi_\pi(u) C_n^{(3/2)}(2u-1) \rightarrow \frac{2(2n+3)}{3(2+n)(1+n)} C_n^{(3/2)}(2u_0-1). \quad (10)$$

Notice that $\tilde{\mu}_\pi \simeq 0$ at tree-level and the corresponding LCDA $\phi_\sigma(u)$ can only be determined by considering the corresponding one-loop expressions (see below). The tree-level solutions (8) fulfill the eom-constraints from (5).

²Notice that there are additional two-gluon LCDA for flavour singlet mesons which we will not consider here, because in the non-relativistic limit glueballs decouple from the $q\bar{q}$ states and the 2-gluon LCDA is only generated by higher-order relativistic corrections. For the definition of the 3-particle LCDAs, see [1, 2].

³This behaviour can also be obtained from the "dense medium limit" in the instanton model [30].

2.3 Definition of LCDAs for heavy pseudoscalar mesons

We define the 2-particle LCDAs of a heavy pseudoscalar B meson following [3, 4],

$$\langle 0 | (\bar{q})_\beta(z) [z, 0] (h_v)_\alpha(0) | B(Mv) \rangle = -\frac{i\hat{f}_B(\mu)M}{4} \left[\frac{1 + \not{v}}{2} \left\{ 2\tilde{\phi}_B^+(t) + \frac{\tilde{\phi}_B^-(t) - \tilde{\phi}_B^+(t)}{t} \not{z} \right\} \gamma_5 \right]_{\alpha\beta}, \quad (11)$$

where v^μ is the heavy meson's velocity, $t \equiv v \cdot z$ and $z^2 = 0$. Here \hat{f}_B is the (renormalization-scale dependent) decay constant in HQET. The Fourier-transformed expressions, which usually appear in factorization formulas, are given through

$$\tilde{\phi}_B^\pm(t) = \int_0^\infty d\omega e^{-i\omega t} \phi_B^\pm(\omega), \quad (12)$$

where ω denotes the light-cone energy of the light quark in the B meson rest frame.

Similarly, according to [31] (see also [32, 33]), the 3-particle LCDAs in coordinate space can be defined as

$$\begin{aligned} & z^\nu \langle 0 | (\bar{q})_\beta(z) [z, uz] gG_{\mu\nu}(uz) [uz, 0] (h_v)_\alpha(0) | B(Mv) \rangle \\ &= \frac{\hat{f}_B(\mu)M}{2} \left[\frac{1 + \not{v}}{2} \left\{ (v_\mu \not{z} - t \gamma_\mu) \left(\tilde{\Psi}_A(t, u) - \tilde{\Psi}_V(t, u) \right) \right. \right. \\ &\quad \left. \left. - i \sigma_{\mu\nu} z^\nu \tilde{\Psi}_V(t, u) - z_\mu \tilde{X}_A(t, u) + \frac{z^\mu}{t} \not{z} \tilde{Y}_A(t, u) \right\} \gamma_5 \right]_{\alpha\beta}, \quad (13) \end{aligned}$$

with the respective Fourier transform

$$\tilde{F}(t, u) = \int_0^\infty d\omega \int_0^\infty d\xi e^{-i(\omega + \xi u)t} F(\omega, \xi), \quad (14)$$

defining the four functions $F = \{\Psi_V, \Psi_A, X_A, Y_A\}$.

2.3.1 Equations of motion

The equations of motion again provide relations between different LCDAs. Including the effect of the 3-particle LCDAs (13), we derive

$$\begin{aligned} & \omega \phi_B^-(\omega) - m \phi_B^+(\omega) + \frac{D-2}{2} \int_0^\omega d\eta [\phi_B^+(\eta) - \phi_B^-(\eta)] \\ &= (D-2) \int_0^\omega d\eta \int_{\omega-\eta}^\infty \frac{d\xi}{\xi} \frac{\partial}{\partial \xi} [\Psi_A(\eta, \xi) - \Psi_V(\eta, \xi)]. \quad (15) \end{aligned}$$

The relation (15) is trivially fulfilled at tree-level and we will show below that it also holds after including the α_s corrections to the NR limit. In [31], Kawamura et al. discuss a second relation which in the massive case reads

$$\begin{aligned} & (\omega + m) \phi_B^-(\omega) + (\omega - 2\bar{\Lambda} - m) \phi_B^+(\omega) \\ &\stackrel{?}{=} -2 \frac{d}{d\omega} \int_0^\omega d\eta \int_{\omega-\eta}^\infty \frac{d\xi}{\xi} [\Psi_A(\eta, \xi) + X_A(\eta, \xi)] - 2(D-2) \int_0^\omega d\eta \int_{\omega-\eta}^\infty \frac{d\xi}{\xi} \frac{\partial \Psi_V(\eta, \xi)}{\partial \xi}, \quad (16) \end{aligned}$$

with $\bar{\Lambda} = M_B - m_b$. We will show below that the equation (16) *does not* hold beyond tree level, since the integral on the right-hand side involving our result for the 3-particle LCDA X_A does not converge. This confirms the criticism raised in [24, 34] that (16) is not consistent, since the renormalization prescription of light-cone operators in HQET and the expansion into local operators do not commute. Notice that in contrast to (15), the derivation of (16) involves derivatives with respect to $z^2 \neq 0$.

If one neglects the 3-particle distribution amplitudes in (15), one arrives at the so-called Wandzura-Wilczek relation which has first been discussed for a massless light quark in [4]. The generalization to the massive case reads

$$\int_0^\omega d\eta [\phi_B^-(\eta) - \phi_B^+(\eta)] \simeq \frac{2}{D-2} [\omega \phi_B^-(\omega) - m \phi_B^+(\omega)] , \quad (17)$$

which again holds for the bare parameters and LCDAs in $D \neq 4$ dimensions.

2.3.2 Tree-level result

By the same arguments as for light mesons, at tree-level the quark and the antiquark in a heavy meson just share the total momentum according to their masses, such that $\omega = m$. In the NR limit, the 2-particle LCDAs of a "heavy" meson are thus given by

$$\phi_B^+(\omega) \simeq \phi_B^-(\omega) \simeq \delta(\omega - m) . \quad (18)$$

Moreover, at tree level, the moments of the heavy meson LCDAs can be related to matrix elements of local operators in HQET [3]. The zeroth moment $\langle 0 | \bar{q} \gamma_5 h_v | B \rangle = -i \hat{f}_B M$ determines the tree-level normalization of the distribution amplitudes $\tilde{\phi}_B^\pm(t=0) \simeq 1$. For the first moment, one has the general decomposition

$$\langle 0 | (\bar{q})_\beta i \overleftarrow{D}^\mu (h_v)_\alpha | B(v) \rangle \simeq -\frac{iM \hat{f}_B}{4} [(av^\mu + b\gamma^\mu) (1 + \psi) \gamma_5]_{\alpha\beta} . \quad (19)$$

Multiplying by $(\gamma_5 \gamma_\mu)_{\beta\alpha}$ and taking into account the finite light quark mass in the NR set-up, the equation of motion for the light quark implies $a + 4b = m$. The equation of motion for the heavy quark is obtained by multiplying with v^μ , from which one obtains $a + b = \bar{\Lambda}$, independent of the light-quark mass. This implies

$$a = \frac{4\bar{\Lambda} - m}{3} , \quad b = -\frac{\bar{\Lambda} - m}{3} .$$

From this we can read off the first moments at tree-level

$$\langle \omega \rangle_+ \simeq \frac{i}{\hat{f}_B M} \langle 0 | \bar{q} \gamma_5 \not{n}_- (i n_- \overleftarrow{D}) h_v | B \rangle = a = \frac{4\bar{\Lambda} - m}{3} , \quad (20)$$

$$\langle \omega \rangle_- \simeq \frac{i}{\hat{f}_B M} \langle 0 | \bar{q} \gamma_5 \not{n}_+ (i n_- \overleftarrow{D}) h_v | B \rangle = 2b + a = \frac{2\bar{\Lambda} + m}{3} , \quad (21)$$

where we introduced the light-like vectors $n_-^\mu = z^\mu/t$ and $n_+^\mu = 2v^\mu - n_-^\mu$. In the non-relativistic limit $\bar{\Lambda} = m$, and we obtain

$$\langle \omega \rangle_\pm \simeq m .$$

Notice that the light-quark mass drops out in the sum

$$\langle \omega \rangle_+ + \langle \omega \rangle_- = 2\bar{\Lambda} .$$

We stress that the relation between moments of $\phi_B^\pm(\omega)$ and local matrix elements in HQET does not hold beyond the tree-level approximation [23, 24, 35].

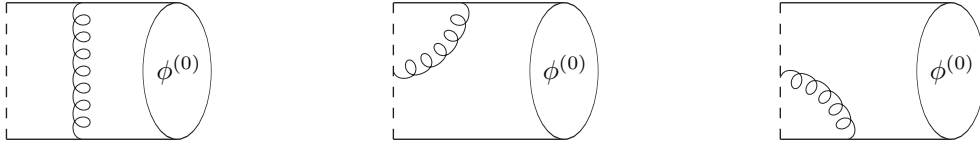


Figure 2: Relativistic corrections to the light-cone distribution amplitudes. The dashed line indicates the Wilson line in the definition of the LCDAs.

3 Relativistic corrections at one-loop

The NR bound states are described by parton configurations with fixed momenta. Relativistic gluon exchange as in Figure 2 leads to modifications: First, there is a correction from matching QCD (or, in the case of heavy mesons, the corresponding low-energy effective theory HQET) on the NR theory. Secondly, there is the usual evolution under the change of the renormalization scale [5, 23]. In particular, the support region for the parton momenta is extended to $0 \leq u \leq 1$ for light mesons and $0 \leq \omega < \infty$ for heavy mesons. In this section we collect the results for LCDAs for “light” and “heavy” mesons including the first-order matching corrections from relativistic gluon exchange

$$\phi_M = \phi_M^{(0)} + \frac{\alpha_s C_F}{4\pi} \phi_M^{(1)} + \mathcal{O}(\alpha_s^2). \quad (22)$$

3.1 Light mesons

3.1.1 Local matrix elements

We first consider the leading-order relativistic corrections to the local matrix elements which are given by the vertex-correction and the wave-function renormalization of the quark fields. We find

$$f_\pi = f_\pi^{\text{NR}} \left[1 + \frac{\alpha_s C_F}{4\pi} \left(-6 + 3 \frac{m_1 - m_2}{m_1 + m_2} \ln \frac{m_1}{m_2} \right) + \mathcal{O}(\alpha_s^2) \right] \quad (23)$$

and

$$\begin{aligned} \mu_\pi &= \frac{m_\pi^2}{Z_{m_1}^{\text{os}} m_1^{\text{os}} + Z_{m_2}^{\text{os}} m_2^{\text{os}}} = m_\pi \left[1 + \frac{\alpha_s C_F}{4\pi} \left(\frac{3}{\varepsilon} + 3 \ln \frac{\mu^2}{m_1 m_2} - 3 \frac{m_1 - m_2}{m_1 + m_2} \ln \frac{m_1}{m_2} + 4 \right) + \mathcal{O}(\alpha_s^2) \right], \\ \tilde{\mu}_\pi &= \mu_\pi - \frac{m_\pi^2}{\mu_\pi} = m_\pi \left[\frac{\alpha_s C_F}{4\pi} \left(\frac{6}{\varepsilon} + 6 \ln \frac{\mu^2}{m_1 m_2} - 6 \frac{m_1 - m_2}{m_1 + m_2} \ln \frac{m_1}{m_2} + 8 \right) + \mathcal{O}(\alpha_s^2) \right], \end{aligned} \quad (24)$$

where $m_\pi \simeq m_1^{\text{os}} + m_2^{\text{os}}$ in the on-shell scheme. Our result for the decay constant is in agreement with [36] and the results for μ_π and $\tilde{\mu}_\pi$ are consistent with the eom-constraints in (6).

3.1.2 The twist-2 LCDA $\phi_\pi(u)$

Let us start with the case of equal quark masses, e.g. in case of a non-relativistic η_c bound state, which may also serve as a toy-model for the pion LCDA.⁴

The first-order relativistic corrections arise from the collinear gluon exchange diagrams in Figure 2, where we also have to take into account the wave-function renormalization of the external quark lines (see Appendix A for details). The local limit of the light-cone matrix element (3) determines the

⁴We should keep in mind, however, that typically non-perturbative analyses from lattice QCD and sum rules find pion distribution amplitudes that are *broader* than the asymptotic one, while the non-relativistic model assumes LCDAs which are *narrower*. Therefore the application of the toy model to the very pion case should not be taken too seriously.

relativistic corrections to the NR decay constant (23) (in this case, the diagrams with the gluon attached to the Wilson-line do not contribute). The remaining contributions to the NLO correction for the leading-twist LCDA contain an UV-divergent piece,

$$\phi_\pi^{(1)}(u)|_{\text{div.}} = \frac{2}{\varepsilon} \int_0^1 dv V(u, v) \phi^{(0)}(v), \quad (25)$$

which involves the well-known Brodsky-Lepage evolution kernel [5],

$$V(u, v) = \left[\left(1 + \frac{1}{v-u} \right) \frac{u}{v} \theta(v-u) + \left(1 + \frac{1}{\bar{v}-\bar{u}} \right) \frac{\bar{u}}{\bar{v}} \theta(u-v) \right]_+. \quad (26)$$

The finite terms after $\overline{\text{MS}}$ -subtraction read

$$\begin{aligned} \phi_\pi^{(1)}(u; \mu) = & 4 \left\{ \left(\ln \frac{\mu^2}{m_\pi^2 (1/2-u)^2} - 1 \right) \left[\left(1 + \frac{1}{1/2-u} \right) u \theta(1/2-u) + (u \leftrightarrow \bar{u}) \right] \right\}_+ \\ & + 4 \left\{ \frac{u(1-u)}{(1/2-u)^2} \right\}_{++}. \end{aligned} \quad (27)$$

Here the plus-distributions are defined as

$$\int_0^1 du \{ \dots \}_+ f(u) \equiv \int_0^1 du \{ \dots \} \left(f(u) - f(1/2) \right), \quad (28)$$

$$\int_0^1 du \{ \dots \}_{++} f(u) \equiv \int_0^1 du \{ \dots \} \left(f(u) - f(1/2) - f'(1/2)(u-1/2) \right). \quad (29)$$

From this it follows that

$$\int_0^1 du \phi_\pi^{(1)}(u; \mu) = \int_0^1 du u \phi_\pi^{(1)}(u; \mu) = 0,$$

such that the general normalization conditions $\int_0^1 du \phi_\pi(u) = 1$ and $\int_0^1 du u \phi_\pi(u) = 1/2$ are not changed. Furthermore, our result for the distribution amplitude obeys the evolution equation

$$\frac{d}{d \ln \mu} \phi_\pi(u; \mu) = \frac{\alpha_s C_F}{\pi} \int_0^1 dv V(u, v) \phi_\pi(v; \mu) + \mathcal{O}(\alpha_s^2). \quad (30)$$

An independent calculation of the leading-twist LCDAs for the η_c and J/ψ meson has been presented in [25]. Our result is not in complete agreement with these findings. In particular, we find that the LCDA quoted in [25] is not normalized to unity as it should be.

On the other hand, at the non-relativistic scale $\mu \simeq m$, the distribution amplitude shows a singular behaviour at $u \simeq u_0 = 1/2$. As a consequence, the convergence of the Gegenbauer expansion is not very good at the non-relativistic scale, with the Gegenbauer coefficients a_n in (10) only falling off as $1/\sqrt{n}$ (and alternating signs). A better characterization of the LCDA at $\mu \simeq m$ is given in terms of the moments

$$\langle \xi^n \rangle_\pi(\mu) \equiv \int_0^1 du (2u-1)^n \phi_\pi(u; \mu), \quad (31)$$

which are linear combinations of Gegenbauer coefficients of order $\leq n$. This corresponds to an expansion of the LCDA in terms of a delta-function and its derivatives,

$$\phi_\pi(u; \mu) = 2 \sum_{n=0}^{\infty} \frac{(-1)^n}{n!} \delta^{(n)}(2u-1) \langle \xi^n \rangle_\pi(\mu). \quad (32)$$

Table 1: The moments $\langle \xi^n \rangle_\pi$ at the non-relativistic scale $\mu = m$.

n	2	4	6	8	10
NR limit	0	0	0	0	0
NLO (27) (for $\alpha_s = 0.2$)	0.067	0.011	0.004	0.002	0.001
v_{NR}^2 (34) (for $v_{\text{NR}}^2 = 0.2$)	0.067	0.008	0.001	0.000	0.000

Results for the first few moments $\langle \xi^n \rangle_\pi$ are shown in Table 1 for the strict non-relativistic limit, including the NLO corrections from (27) and comparing with the non-relativistic corrections of order v_{NR}^2 discussed by Braguta et al. in [26]. Keeping first-order corrections in v_{NR}^2 only, this formally amounts to the replacement

$$\phi_\pi^{\text{NR}}(u) = \delta(u - 1/2) + \frac{v_{\text{NR}}^2}{24} \delta''(u - 1/2) + \mathcal{O}(v_{\text{NR}}^4). \quad (33)$$

In particular, this fixes the moment $\langle \xi^2 \rangle_\pi = \frac{v_{\text{NR}}^2}{3}$. The authors [26] propose a resummed formula,

$$\phi_\pi^{\text{NR}}(u) \rightarrow \frac{1}{v_{\text{NR}}} \theta\left(u - \frac{1 - v_{\text{NR}}}{2}\right) \theta\left(\frac{1 + v_{\text{NR}}}{2} - u\right). \quad (34)$$

The comparison in Table 1 shows that for $v_{\text{NR}}^2 \simeq \alpha_s(m) \simeq 0.2$, the effect of the v_{NR}^2 corrections is qualitatively and quantitatively similar to the α_s corrections from (27).

It is also interesting to determine the correction to the first inverse moment of the LCDA which appears in QCD factorization formulas

$$\langle u^{-1} \rangle_\pi^{(1)}(\mu) \equiv \int_0^1 du \frac{\phi_\pi^{(1)}(u; \mu)}{u} \simeq 3 \left(2.73 + 1.08 \ln \frac{\mu^2}{m^2} \right). \quad (35)$$

Finally, we quote the result for the derivative of $\phi_\pi(u)$ at the endpoints

$$\phi'_\pi(0; \mu) = -\phi'_\pi(1; \mu) = \frac{\alpha_s C_F}{4\pi} \left(4 + 12 \ln \frac{\mu^2}{m^2} \right) + \mathcal{O}(\alpha_s^2), \quad (36)$$

which is sometimes discussed in the context of non-factorizable contributions to hard exclusive reactions [37, 38].

For non-equal quark masses, the NLO corrections to the $\overline{\text{MS}}$ -renormalized twist-2 LCDA are given by

$$\begin{aligned} \phi_K^{(1)}(u; \mu) = & 2 \left\{ \left(\ln \frac{\mu^2}{m_K^2 (u_0 - u)^2} - 1 \right) \left[\left(1 + \frac{1}{u_0 - u} \right) \frac{u}{u_0} \theta(u_0 - u) + \left(\begin{array}{c} u \leftrightarrow \bar{u} \\ u_0 \leftrightarrow \bar{u}_0 \end{array} \right) \right] \right\}_+ \\ & + 4 \left\{ \frac{u(1-u)}{(u_0 - u)^2} \right\}_{++} + 2 \delta'(u - u_0) \left(2u_0(1 - u_0) \ln \frac{u_0}{1 - u_0} + 2u_0 - 1 \right). \end{aligned} \quad (37)$$

The first moment now becomes

$$\int_0^1 du u \phi_K(u; \mu) = u_0 + \frac{\alpha_s C_F}{4\pi} \left[\left(-\frac{4}{3} \ln \frac{\mu^2}{u_0^2 m_K^2} - \frac{7(1 - u_0)}{3} \ln u_0^2 - \frac{38}{9} \right) u_0 - (u_0 \leftrightarrow \bar{u}_0) \right]. \quad (38)$$

3.1.3 2-particle LCDAs of twist-3

The twist-3 LCDAs for the 2-particle Fock states are obtained in the same way as the twist-2 one. After absorbing the corrections to the local matrix elements into the renormalized values for μ_π and $\tilde{\mu}_\pi$, we obtain a UV-divergent piece

$$\phi_p^{(1)}(u)|_{\text{div.}} = \frac{2}{\varepsilon} \left[\left(1 + \frac{1}{u_0 - u} \right) \theta(u_0 - u) + \left(\begin{array}{c} u \leftrightarrow \bar{u} \\ u_0 \leftrightarrow \bar{u}_0 \end{array} \right) \right]_+ \quad (39)$$

and a finite NLO contribution to the twist-3 LCDA associated to the pseudoscalar current

$$\begin{aligned} \phi_p^{(1)}(u; \mu) = & 2 \left\{ \left(\ln \frac{\mu^2}{m_K^2 (u_0 - u)^2} - 1 \right) \left[\left(1 + \frac{1}{u_0 - u} \right) \theta(u_0 - u) + \left(\begin{array}{c} u \leftrightarrow \bar{u} \\ u_0 \leftrightarrow \bar{u}_0 \end{array} \right) \right] \right\}_+ \\ & + 4u_0(1 - u_0) \left(\left\{ \frac{1}{(u_0 - u)^2} \right\}_{++} + \delta'(u - u_0) \ln \frac{u_0}{1 - u_0} \right) + 2 \left\{ \frac{2u_0 - 1}{(u_0 - u)} \right\}_+. \end{aligned} \quad (40)$$

In particular, the first moment of $\phi_p(u)$ now reads

$$\int_0^1 du u \phi_p(u; \mu) = u_0 + \frac{\alpha_s C_F}{4\pi} \left[\left(-3 \ln \frac{\mu^2}{m_K^2} + 6u_0 \ln u_0 - 4 \right) u_0 - (u_0 \leftrightarrow \bar{u}_0) \right], \quad (41)$$

which is in agreement with the eom-constraint from (7). At the endpoints we now have

$$\phi_p(0; \mu) = \frac{\alpha_s C_F}{4\pi} \left(\frac{2 + 2u_0}{u_0} \ln \frac{\mu^2}{m_1^2} - 2 \right) + \mathcal{O}(\alpha_s^2) \quad (42)$$

and similar for $\phi_p(1; \mu)$ with $m_1 \leftrightarrow m_2$, i.e. $u_0 \leftrightarrow \bar{u}_0$. For the twist-3 LCDA associated to the pseudotensor current (whose normalization factor starts at order α_s), we simply have

$$\phi_\sigma(u) = 2 \left[\frac{u}{u_0} \theta(u_0 - u) + \left(\begin{array}{c} u \leftrightarrow \bar{u} \\ u_0 \leftrightarrow \bar{u}_0 \end{array} \right) \right] + \mathcal{O}(\alpha_s). \quad (43)$$

In contrast to the other 2-particle LCDAs in (8), we find that $\phi_\sigma(u)$ is not given by a delta-like distribution in the NR limit and has support for $0 \leq u \leq 1$.

3.2 Heavy mesons

The calculation of the LCDAs for a B_c meson (which again can be considered as a toy model for LCDAs of B_q mesons with $m_b \gg m_q$) goes along the same lines as for the η_c case. However, important differences arise because the heavy b -quark is to be treated in HQET which modifies the divergence structure of the loop integrals (notice that in our set-up, a charm quark in a B_c meson is treated as "light"). As a consequence, the evolution equations for the LCDAs of heavy mesons [23] differ from those of light mesons.

3.2.1 The LCDA $\phi_B^+(\omega)$

Let us first focus on the distribution amplitude $\phi_B^+(\omega)$ which enters the QCD factorization formulas for exclusive heavy-to-light decays. In the local limit we derive the corrections from soft gluon exchange to the decay constant in HQET. We find

$$\hat{f}_M(\mu) = f_M^{\text{NR}} \left[1 + \frac{\alpha_s C_F}{4\pi} \left(3 \ln \frac{\mu}{m} - 4 \right) + \mathcal{O}(\alpha_s^2) \right]. \quad (44)$$

Notice that the decay constant of a heavy meson exhibits the well-known scale dependence in HQET [39]. The remaining NLO corrections to the distribution amplitude $\phi_B^+(\omega)$ contain an UV-divergent piece (details of the derivation can be found in Appendix B)

$$\phi_B^{(+,1)}(\omega; \mu)|_{\text{div.}} = \frac{2\omega}{\epsilon} \left[\frac{\theta(m-\omega)}{m(m-\omega)} + \frac{\theta(\omega-m)}{\omega(\omega-m)} \right]_+ - \delta(\omega-m) \left[\frac{1}{\epsilon^2} - \frac{1}{\epsilon} \left(1 - \ln \frac{\mu^2}{m^2} \right) \right] \quad (45)$$

and a finite piece

$$\begin{aligned} \frac{\phi_B^{(+,1)}(\omega; \mu)}{\omega} &= 2 \left[\left(\ln \left[\frac{\mu^2}{(\omega-m)^2} \right] - 1 \right) \left(\frac{\theta(m-\omega)}{m(m-\omega)} + \frac{\theta(\omega-m)}{\omega(\omega-m)} \right) \right]_+ + 4 \left[\frac{\theta(2m-\omega)}{(\omega-m)^2} \right]_{++} \\ &+ \frac{4\theta(\omega-2m)}{(\omega-m)^2} - \frac{\delta(\omega-m)}{m} \left(\frac{1}{2} \ln^2 \frac{\mu^2}{m^2} - \ln \frac{\mu^2}{m^2} + \frac{3\pi^2}{4} + 2 \right) \end{aligned} \quad (46)$$

with an analogous definition of plus-distributions as in (28,29). Notice that, in order to separate the UV divergence coming from the longitudinal momentum integration, we have introduced an auxiliary parameter $\mu_f \equiv 2m$ to split the support region of the LCDA into two parts. The distribution amplitude in (46) obeys the evolution equation

$$\frac{d}{d \ln \mu} \phi_B^+(\omega; \mu) = -\frac{\alpha_s C_F}{4\pi} \int_0^\infty d\omega' \gamma_+^{(1)}(\omega, \omega'; \mu) \phi_B^+(\omega'; \mu) + \mathcal{O}(\alpha_s^2), \quad (47)$$

where the anomalous dimension $\gamma_+^{(1)}(\omega, \omega'; \mu)$ can be read off the UV-divergent terms in (45) and is given by [23]

$$\gamma_+^{(1)}(\omega, \omega'; \mu) = \left(\Gamma_{\text{cusp}}^{(1)} \ln \frac{\mu}{\omega} - 2 \right) \delta(\omega - \omega') - \Gamma_{\text{cusp}}^{(1)} \omega \left[\frac{\theta(\omega' - \omega)}{\omega'(\omega' - \omega)} + \frac{\theta(\omega - \omega')}{\omega(\omega - \omega')} \right]_+ \quad (48)$$

with $\Gamma_{\text{cusp}}^{(1)} = 4$.

In contrast to the light meson case, the normalization of the heavy meson distribution amplitude is ill-defined. Imposing a hard cutoff $\Lambda_{\text{UV}} \gg m$ and expanding to first order in m/Λ_{UV} , we find

$$\int_0^{\Lambda_{\text{UV}}} d\omega \phi_B^+(\omega; \mu) \simeq 1 - \frac{\alpha_s C_F}{4\pi} \left[\frac{1}{2} \ln^2 \frac{\mu^2}{\Lambda_{\text{UV}}^2} + \ln \frac{\mu^2}{\Lambda_{\text{UV}}^2} + \frac{\pi^2}{12} \right] + \mathcal{O}(\alpha_s^2) + \mathcal{O}(m/\Lambda_{\text{UV}}) \quad (49)$$

and similarly for the first moment

$$\frac{1}{\Lambda_{\text{UV}}} \int_0^{\Lambda_{\text{UV}}} d\omega \omega \phi_B^+(\omega; \mu) \simeq \frac{\alpha_s C_F}{4\pi} \left[2 \ln \frac{\mu^2}{\Lambda_{\text{UV}}^2} + 6 \right] + \mathcal{O}(\alpha_s^2) + \mathcal{O}(m/\Lambda_{\text{UV}}). \quad (50)$$

The last two expressions provide model-independent properties of the distribution amplitude which have been studied within the operator product expansion in [35]. Our results are in agreement with these general findings.

We finally quote our result for two phenomenologically relevant moments in the factorization approach to heavy-to-light decays [24, 35]

$$(\lambda_B(\mu))^{-1} \equiv \int_0^\infty d\omega \frac{\phi_B^+(\omega; \mu)}{\omega} = \frac{1}{m} \left(1 - \frac{\alpha_s C_F}{4\pi} \left[\frac{1}{2} \ln^2 \frac{\mu^2}{m^2} - \ln \frac{\mu^2}{m^2} + \frac{3\pi^2}{4} - 2 \right] \right) + \mathcal{O}(\alpha_s^2), \quad (51)$$

and

$$\sigma_B(\mu) \equiv \sigma_B^{(1)}(\mu) = \ln \frac{\mu}{m} + \frac{\alpha_s C_F}{4\pi} [8\zeta_3] + \mathcal{O}(\alpha_s^2), \quad (52)$$

where $\zeta_j = \sum_{n=1}^{\infty} n^{-j}$ is the Riemann zeta function and we defined

$$\sigma_B^{(n)}(\mu) \equiv \lambda_B(\mu) \int_0^{\infty} d\omega \frac{\phi_B^+(\omega; \mu)}{\omega} \left[\ln \frac{\mu}{\omega} \right]^n. \quad (53)$$

The leading-order scale-dependence of these quantities is in general given by

$$\frac{d\lambda_B^{-1}}{d \ln \mu} = -\frac{\alpha_s C_F}{4\pi} \left(\Gamma_{\text{cusp}}^{(1)} \sigma_B - 2 \right) \lambda_B^{-1} + \mathcal{O}(\alpha_s^2), \quad (54)$$

$$\frac{d\sigma_B}{d \ln \mu} = 1 + \frac{\alpha_s C_F}{4\pi} \Gamma_{\text{cusp}}^{(1)} \left((\sigma_B)^2 - \sigma_B^{(2)} \right) + \mathcal{O}(\alpha_s^2). \quad (55)$$

In particular, in the non-relativistic limit $\sigma_B^{(n)}(\mu) = (\sigma_B(\mu))^n$ and therefore the α_s correction on the right hand side of (52) does not depend explicitly on $\ln \mu$. For arbitrary values of n , we find for the scale dependence of the logarithmic moments

$$\frac{d\sigma_B^{(n)}}{d \ln \mu} = n\sigma_B^{(n-1)} + \frac{\alpha_s C_F}{4\pi} \Gamma_{\text{cusp}}^{(1)} \left[\sigma_B^{(1)} \sigma_B^{(n)} - \sigma_B^{(n+1)} + 2n! \sum_{j=1}^{[n/2]} \frac{\zeta_{2j+1}}{(n-2j)!} \sigma_B^{(n-2j)} \right] + \mathcal{O}(\alpha_s^2), \quad (56)$$

where $[x]$ denotes the greatest integer less than or equal to x .

3.2.2 The LCDA $\phi_B^-(\omega)$

A similar analysis can be performed for the other 2-particle LCDA of the B meson. We now obtain for the UV-divergent piece (see also Appendix B)

$$\begin{aligned} \phi_B^{(-,1)}(\omega; \mu)|_{\text{div.}} &= \frac{2}{\epsilon} \left[\frac{\theta(m-\omega)}{(m-\omega)} \right]_+ + \frac{2}{\epsilon} \frac{\theta(m-\omega)}{m} + \frac{2\omega}{\epsilon} \left[\frac{\theta(\omega-m)}{\omega(\omega-m)} \right]_+ \\ &\quad - \delta(\omega-m) \left[\frac{1}{\epsilon^2} + \frac{1}{\epsilon} \left(1 + \ln \frac{\mu^2}{m^2} \right) \right]. \end{aligned} \quad (57)$$

The finite contributions read

$$\begin{aligned} \phi_B^{(-,1)}(\omega; \mu) &= 2 \left[\left(\ln \left[\frac{\mu^2}{(\omega-m)^2} \right] - 1 \right) \frac{\theta(m-\omega)}{m-\omega} \right]_+ + 2 \left(\ln \left[\frac{\mu^2}{(\omega-m)^2} \right] - 1 \right) \frac{\theta(m-\omega)}{m} \\ &\quad + 2\omega \left[\left(\ln \left[\frac{\mu^2}{(\omega-m)^2} \right] - 1 \right) \frac{\theta(\omega-m)}{\omega(\omega-m)} \right]_+ + 4m \left[\frac{\theta(2m-\omega)}{(\omega-m)^2} \right]_{++} \\ &\quad + 4m \frac{\theta(\omega-2m)}{(\omega-m)^2} - \delta(\omega-m) \left(\frac{1}{2} \ln^2 \frac{\mu^2}{m^2} + \ln \frac{\mu^2}{m^2} + \frac{3\pi^2}{4} + 6 \right). \end{aligned} \quad (58)$$

The distribution amplitude in (58) obeys the evolution equation

$$\begin{aligned} \frac{d}{d \ln \mu} \phi_B^-(\omega; \mu) &= -\frac{\alpha_s C_F}{4\pi} \int_0^{\infty} d\omega' \gamma_-^{(1)}(\omega, \omega'; \mu) \phi_B^-(\omega'; \mu) \\ &\quad - \frac{\alpha_s C_F}{4\pi} \int_0^{\infty} d\omega' \gamma_{-+}^{(1)}(\omega, \omega'; \mu) \phi_B^+(\omega'; \mu) + \mathcal{O}(\alpha_s^2), \end{aligned} \quad (59)$$

where the anomalous dimension kernels $\gamma_-^{(1)}(\omega, \omega'; \mu)$ and $\gamma_{-+}^{(1)}(\omega, \omega'; \mu)$ can be read off the UV-divergent terms in (57) (see Appendix B for details)

$$\gamma_-^{(1)}(\omega, \omega'; \mu) = \gamma_+^{(1)}(\omega, \omega'; \mu) - \Gamma_{\text{cusp}}^{(1)} \frac{\theta(\omega' - \omega)}{\omega'}, \quad (60)$$

$$\gamma_{-+}^{(1)}(\omega, \omega'; \mu) = -\Gamma_{\text{cusp}}^{(1)} \left[\frac{m\theta(\omega' - \omega)}{\omega'^2} \right]_+. \quad (61)$$

Among others, the knowledge of γ_- is essential to check the factorization of certain correlation functions appearing in sum-rule calculations for $B \rightarrow \pi$ form factors within SCET [40].

Another new result are the first positive moments of the LCDA $\phi_B^-(\omega)$ as a function of a hard cutoff $\Lambda_{\text{UV}} \gg m$,

$$\int_0^{\Lambda_{\text{UV}}} d\omega \phi_B^-(\omega; \mu) \simeq 1 - \frac{\alpha_s C_F}{4\pi} \left[\frac{1}{2} \ln^2 \frac{\mu^2}{\Lambda_{\text{UV}}^2} - \ln \frac{\mu^2}{\Lambda_{\text{UV}}^2} + \frac{\pi^2}{12} \right] + \mathcal{O}(\alpha_s^2) + \mathcal{O}(m/\Lambda_{\text{UV}}), \quad (62)$$

$$\frac{1}{\Lambda_{\text{UV}}} \int_0^{\Lambda_{\text{UV}}} d\omega \omega \phi_B^-(\omega; \mu) \simeq \frac{\alpha_s C_F}{4\pi} \left[2 \ln \frac{\mu^2}{\Lambda_{\text{UV}}^2} + 2 \right] + \mathcal{O}(\alpha_s^2) + \mathcal{O}(m/\Lambda_{\text{UV}}), \quad (63)$$

which are again expected to be model-independent. Actually, these moments can already be derived in the Wandzura-Wilczek approximation. From the solution of (17) in $D = 4 - 2\epsilon$ dimensions

$$\phi_B^-(\omega; \mu) = (1 - \epsilon) \int_\omega^\infty d\eta \frac{\eta - m}{\eta^2} \left(\frac{\eta}{\omega} \right)^\epsilon \phi_B^+(\eta; \mu) + \frac{m}{\omega} \phi_B^+(\omega; \mu), \quad (64)$$

we obtain the bare (unrenormalized) moments

$$\langle \omega^n \rangle_B^- \simeq \frac{\Lambda^{n+1} \phi_B^-(\Lambda) + (1 - \epsilon) \langle \omega^n \rangle_B^+}{n + 1 - \epsilon}, \quad (65)$$

which result in the same $\overline{\text{MS}}$ -subtracted moments as in (62,63), i.e. the 3-particle LCDAs only contribute subleading terms to these moments in our case.

We finally quote the quantity

$$\phi_B^-(0; \mu) = \frac{\alpha_s C_F}{4\pi} \frac{4}{m} \ln \frac{\mu^2}{m^2} + \mathcal{O}(\alpha_s^2), \quad (66)$$

which plays a role in sum-rule calculations for heavy-to-light form factors [40, 41].

3.2.3 3-particle LCDAs and equations of motion

In order to verify whether the equations of motion (15,16) hold after including first order relativistic corrections, we have to compute the 3-particle LCDAs which arise at order α_s in the non-relativistic limit. Without going into details, we quote our results for the bare LCDAs that enter (15,16)

$$\begin{aligned} \Psi_V(\omega, \xi) &= \frac{\alpha_s C_F}{4\pi} \frac{\delta(\omega - m + \xi)}{2m} \left\{ \left(\frac{1}{\epsilon} + \ln \frac{\mu^2}{\xi^2} - 1 \right) \xi^2 \theta(m - \xi) - \left(\frac{1}{\epsilon} + \ln \frac{\mu^2}{m^2} + 1 \right) m^3 \delta(\xi - m) \right\}, \\ \Psi_A(\omega, \xi) &= \frac{\alpha_s C_F}{4\pi} \frac{\delta(\omega - m + \xi)}{2m} \left\{ - \left(\frac{1}{\epsilon} + \ln \frac{\mu^2}{\xi^2} + 1 \right) \xi^2 \theta(m - \xi) - \left(\frac{1}{\epsilon} + \ln \frac{\mu^2}{m^2} + 1 \right) m^3 \delta(\xi - m) \right\}, \\ X_A(\omega, \xi) &= \frac{\alpha_s C_F}{4\pi} \left[2 \left(\frac{1}{\epsilon} + \ln \frac{\mu^2}{\xi^2} \right) \xi \delta(\omega - m) - \frac{\delta(\omega - m + \xi)}{2m} \right. \\ &\quad \left. \left\{ \left[(4m - 3\xi) \left(\frac{1}{\epsilon} + \ln \frac{\mu^2}{\xi^2} \right) - \xi \right] \xi \theta(m - \xi) - \left(\frac{1}{\epsilon} + \ln \frac{\mu^2}{m^2} + 1 \right) m^3 \delta(\xi - m) \right\} \right]. \quad (67) \end{aligned}$$

We show in Appendix C that the eom-constraint (15) is indeed fulfilled to order α_s . On the other hand we find that (16) *does not* hold beyond tree level since the ξ -integral involving our result for the 3-particle LCDA X_A is ill-defined for $\xi \rightarrow \infty$. Since we again expect the radiative tail of the 3-particle LCDAs (which determines the large- ξ behaviour) to be model-independent, the failure of (16) beyond tree level should be considered a general feature.

Table 2: The moments $\langle \xi^n \rangle_\pi$ as a function of the evolution parameter $\eta = \alpha_s(\mu)/\alpha_s(m)$.

n	2	4	6	8	10
LL ($\eta = 1/5$)	0.126	0.048	0.025	0.015	0.010
LL ($\eta = 1/25$)	0.173	0.070	0.038	0.024	0.016
asymptotic	0.200	0.086	0.048	0.030	0.021

4 Renormalization-group evolution

In physical applications, the light-cone distribution amplitudes are required at the hard-scattering scale μ which is set by the momentum transfer in the exclusive reaction. The evolution from the “soft” scale m to the hard-scattering scale μ resums large logarithms $\ln \mu^2/m^2$. In this section we study the evolution of the NR distribution amplitudes to leading logarithmic (LL) approximation. For “light” mesons we focus on the twist-2 LCDA $\phi_\pi(u)$ and for “heavy” mesons we consider the 2-particle LCDAs $\phi_B^+(\omega)$ and $\phi_B^-(\omega)$.

4.1 The twist-2 LCDA $\phi_\pi(u)$

The evolution of the twist-2 LCDA $\phi_\pi(u; \mu)$ is described by the Brodsky-Lepage kernel (26). To solve the evolution equation (30), one projects the distribution amplitude onto Gegenbauer polynomials (9) which are eigenfunctions of the LO evolution kernel. The respective coefficients are obtained from (10) and have the LL evolution

$$a_n(\mu) = a_n(\mu_0) \left(\frac{\alpha_s(\mu)}{\alpha_s(\mu_0)} \right)^{-\gamma_n/\beta_0}, \quad \gamma_n = C_F \left(3 + \frac{2}{(n+1)(n+2)} - 4 \sum_{j=1}^{n+1} \frac{1}{j} \right), \quad (68)$$

with $\beta_0 = (33 - 2n_f)/3$ (for illustration, we will use $n_f = 3$ in the numerical examples). For very large $n \gg 1$ we have $\gamma_n \simeq -4C_F \ln n$, which implies that the effect of higher Gegenbauer coefficients becomes less important at high scales. Notice that the result for the LL evolution only depends on the ratio of coupling constants $\eta(\mu) = \frac{\alpha_s(\mu)}{\alpha_s(\mu_0)}$, irrespective of the individual values for μ and μ_0 .

We show in Table 2 the LL evolution of the moments $\langle \xi^n \rangle_\pi$ defined in (31), starting from the tree-level result in the NR limit, $\phi_\pi(u; \mu_0 = m) = \delta(u - 1/2)$, for two values of $\eta = \alpha_s(\mu)/\alpha_s(m)$ and in the asymptotic limit. In contrast to the moments $\langle \xi^n \rangle_\pi$, the phenomenologically important $1/u$ moment is a linear combination of an *infinite* number of Gegenbauer moments,

$$\langle u^{-1} \rangle_\pi(\mu) = 3 \sum_{j=0}^{\infty} a_{2j}(\mu). \quad (69)$$

In order to study the evolution effects from the non-relativistic scale, where $\langle u^{-1} \rangle_\pi(\mu_0 = m) = 2$, towards $\mu \gg m$, it will therefore be crucial to control the effects of higher Gegenbauer coefficients. For this purpose, we find it convenient to consider model parameterizations which are obtained from a slight modification of the strategy developed in [42]. Our ansatz involves three real parameters $a > 0$, $b > 0$, $0 \leq t_c \leq 1$,

$$\phi_\pi(u) \equiv \frac{3u\bar{u}}{\Gamma(a; -\ln t_c)} \int_0^{t_c} dt (-\ln t)^{a-1} \left[f(2u-1, it^{1/b}) + f(2u-1, -it^{1/b}) \right] \quad (70)$$

with $\Gamma(a; b) = \int_b^\infty dt t^{a-1} e^{-t}$ and the generating function of the Gegenbauer polynomials,

$$f(\xi, \theta) = \frac{1}{(1 - 2\xi\theta + \theta^2)^{3/2}} = \sum_{n=0}^{\infty} C_n^{3/2}(\xi) \theta^n. \quad (71)$$

Performing the t -integration in (70), one finds

$$\phi_\pi(u) = 6u\bar{u} \sum_{n=0}^{\infty} \left[\cos\left(\frac{n\pi}{2}\right) \frac{\Gamma(a; -(1+n/b) \ln t_c)}{\Gamma(a; -\ln t_c)} (n/b + 1)^{-a} \right] C_n^{3/2}(2u-1), \quad (72)$$

from which one reads off the Gegenbauer coefficients $a_{\text{odd}} = 0$ and

$$a_n = \frac{(-1)^{n/2}}{(n/b + 1)^a} \frac{\Gamma(a; -(1+n/b) \ln t_c)}{\Gamma(a; -\ln t_c)} \quad \text{for } n \text{ even.} \quad (73)$$

For $t_c \rightarrow 0$ our ansatz reduces to the asymptotic distribution amplitude and for $t_c \rightarrow 1$ it is equivalent to one of the models discussed in [42], where the Gegenbauer coefficients show a simple power-like fall-off (in this case with alternating signs). As observed in [42], for values of $a \leq 3$, the model induces some pathological behaviour at $u = 1/2$. In our ansatz this is regularized by the cut-off parameter $t_c < 1$. The qualitative behaviour of the Gegenbauer coefficients for large n now depends on t_c :

- For moderately large values of n , we have

$$1 \ll n \ll n_{\text{crit}} \equiv -b(1 + 1/\ln t_c) \quad : \quad |a_n| \simeq (n/b)^{-a}, \quad (74)$$

i.e. a power-like fall-off with n as in [42].

- For asymptotically large values of n , one obtains

$$n \gg n_{\text{crit}} : \quad |a_n| \simeq \frac{b(-\ln t_c)^{a-1}}{\Gamma(a; -\ln t_c)} \frac{t_c^{n/b}}{n}, \quad (75)$$

i.e. an exponential fall-off with n , which renders the contribution of *very* high Gegenbauer coefficients irrelevant.

We now reconsider the evolution of the tree-level result in the NR limit $\phi_\pi(u; \mu_0 = m) = \delta(u-1/2)$ and fix the model parameters (a, b, t_c) in (70) from the first three non-vanishing Gegenbauer coefficients using (10),

$$\left. \begin{array}{l} a_2(m) \simeq -0.5833 \\ a_4(m) \simeq +0.4583 \\ a_6(m) \simeq -0.3906 \end{array} \right\} \Rightarrow \begin{array}{l} a \simeq 0.3962 \\ b \simeq 0.8045 \\ t_c \simeq 0.9993 \\ n_{\text{crit}} \simeq 1149 \end{array} \quad (76)$$

The fact that $a < 1$ and $n_{\text{crit}} \gg 1$ reflects the bad convergence of the Gegenbauer expansion in the NR limit. Still, the model parameterization reproduces the Gegenbauer coefficients with $n \ll n_{\text{crit}}$ and the value of the first inverse moment $\langle u^{-1} \rangle_\pi$ to a very good accuracy (see the first line in Table 3).

The same strategy can be applied for scales $\mu > m$. The LL evolution towards larger scales depends on $\eta_i = \alpha_s(\mu_i)/\alpha_s(m)$. For illustration, we consider $\eta_1 = 1/5$ and $\eta_2 = 1/25$ and obtain

$$\left. \begin{array}{l} a_2(\mu_1) \simeq -0.2160 \\ a_4(\mu_1) \simeq +0.1079 \\ a_6(\mu_1) \simeq -0.0679 \end{array} \right\} \Rightarrow \begin{array}{l} a \simeq 1.2679 \\ b \simeq 0.8708 \\ t_c \simeq 0.9811 \\ n_{\text{crit.}} \simeq 45 \end{array} \quad (77)$$

and

$$\left. \begin{array}{l} a_2(\mu_2) \simeq -0.0800 \\ a_4(\mu_2) \simeq +0.0254 \\ a_6(\mu_2) \simeq -0.0118 \end{array} \right\} \Rightarrow \begin{array}{l} a \simeq 2.1451 \\ b \simeq 0.8966 \\ t_c \simeq 0.9418 \\ n_{\text{crit.}} \simeq 14 \end{array} \quad (78)$$

Table 3: LL evolution of the first few Gegenbauer coefficients starting from the NR distribution amplitude $\phi_\pi(u) = \delta(u - 1/2)$. For each value of the evolution parameter $\eta = \alpha_s(\mu)/\alpha_s(m)$ we show the results for the exact expression, the model parameterization (70) and a truncated conformal expansion (9) with $n \leq 6$. We also quote the value for the first inverse moment $\langle u^{-1} \rangle_\pi$.

	a_2	a_4	a_6	a_8	a_{10}	a_{12}	a_{14}	a_{16}	$\langle u^{-1} \rangle_\pi$
exact ($\eta = 1$)	-0.583	0.458	-0.391	0.346	-0.314	0.290	-0.271	0.255	
model	*	*	*	0.346	-0.314	0.289	-0.269	0.253	2.00
conformal exp.	*	*	*	(truncation $n \leq 6$)					1.45
exact ($\eta = 1/5$)	-0.216	0.108	-0.068	0.048	-0.036	0.029	-0.023	0.020	
model	*	*	*	0.048	-0.036	0.028	-0.023	0.019	2.55
conformal exp.	*	*	*	(truncation $n \leq 6$)					2.47
exact ($\eta = 1/25$)	-0.080	0.025	-0.012	0.007	-0.004	0.003	-0.002	0.002	
model	*	*	*	0.007	-0.004	0.003	-0.002	0.001	2.81
conformal exp.	*	*	*	(truncation $n \leq 6$)					2.80

We observe that the parameter a increases under evolution, which is related to the growth of the anomalous dimensions for larger values of n , leading to a steeper fall-off of the Gegenbauer coefficients at larger scales. Effectively, for moderately large values of n , one has

$$a(\mu_i) \approx a(m) - \frac{4C_F}{\beta_0} \ln \eta_i. \quad (79)$$

The parameter b is only slightly increasing while t_c is decreasing under evolution. The critical value of n is quickly decreasing from $n_{\text{crit}} \simeq 1149$ at $\mu = m$ to $n_{\text{crit}} \simeq 14$ at $\mu = \mu_2$. Figure 3 shows the evolution of the model LCDA as a function of u . For $\eta = 1/5$ the functional form still “remembers” the non-relativistic profile, while for $\eta = 1/25$ it is already close to the asymptotic form. Table 3 compares the first few Gegenbauer coefficients using the exact projection of the delta-function and the model parameterization (70). We see that the differences are tiny and the model gives a good approximation. We also quote the result for the first inverse moment which slowly evolves from the NR value, $\langle u^{-1} \rangle_\pi(\mu_0 = m) = 2$, towards the asymptotic value $\langle u^{-1} \rangle_\pi(\mu \rightarrow \infty) = 3$. We clearly see that the model gives a better description for relatively low scales than a truncated conformal expansion (9) with $n \leq 6$ (i.e. with the same number of input parameters as our model). The latter can be improved, however, by considering the averaged moment

$$\langle u^{-1} \rangle_\pi(\mu) \simeq \frac{3}{2} \left(\sum_{j=0}^{j_{\text{max}}} a_{2j}(\mu) + \sum_{j=0}^{j_{\text{max}}-1} a_{2j}(\mu) \right), \quad (80)$$

which accounts for the alternating sign behaviour of the Gegenbauer coefficients. Using this improved truncated conformal expansion, we find that the $1/u$ moment is given by $\langle u^{-1} \rangle_\pi = (2.04, 2.57, 2.82)$ at respective scales (m, μ_1, μ_2) , which is very similar to the predictions of the model parameterization (see Table 3).

4.2 The LCDA $\phi_B^\pm(\omega)$

The evolution of the LCDA $\phi_B^\pm(\omega; \mu)$ for scales $m \leq \mu \leq M$ is described by the Lange-Neubert kernel (48).⁵ The solution of the evolution equation (47) can be written in closed form as [35]

$$\phi_B^\pm(\omega; \mu) = e^{V-2\gamma_E g} \frac{\Gamma(2-g)}{\Gamma(g)} \int_0^\infty \frac{d\omega'}{\omega'} \phi_B^\pm(\omega'; \mu_0) \left(\frac{\omega_{>}}{\mu_0} \right)^g \frac{\omega_{<}}{\omega_{>}} {}_2F_1 \left(1-g, 2-g; 2; \frac{\omega_{<}}{\omega_{>}} \right), \quad (81)$$

⁵Notice that above the b -quark mass scale one should match the LCDAs in HQET onto LCDAs in QCD, see e.g. [43].

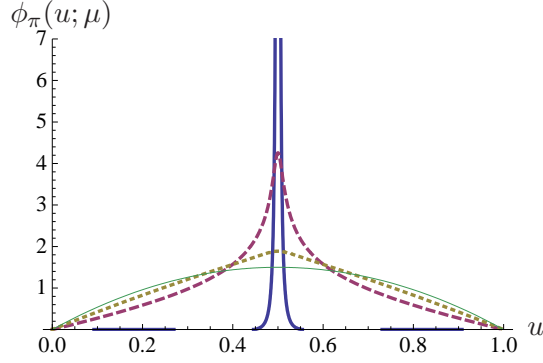


Figure 3: Approximation of the NR distribution amplitude $\phi_\pi(u) = \delta(u - 1/2)$ in terms of the model parameterization (70) (thick solid line) and its evolution for $\eta = 1/5$ (dashed line) and $\eta = 1/25$ (dotted line). The asymptotic LCDA is shown for comparison (thin solid line).

where $\omega_< = \min(\omega, \omega')$ and $\omega_> = \max(\omega, \omega')$. The evolution is controlled by the functions

$$V \equiv V(\mu, \mu_0) = - \int_{\alpha_s(\mu_0)}^{\alpha_s(\mu)} \frac{d\alpha}{\beta(\alpha)} \left[\Gamma_{\text{cusp}}(\alpha) \int_{\alpha_s(\mu_0)}^{\alpha} \frac{d\alpha'}{\beta(\alpha')} + \gamma(\alpha) \right], \quad (82)$$

with $\Gamma_{\text{cusp}} \simeq \frac{\alpha_s C_F}{\pi}$, $\gamma \simeq -\frac{\alpha_s C_F}{2\pi}$, $\beta \simeq -\frac{\alpha_s^2 \beta_0}{2\pi}$ (we use $n_f = 4$ in the numerical examples) and

$$g \equiv g(\mu, \mu_0) = \int_{\alpha_s(\mu_0)}^{\alpha_s(\mu)} d\alpha \frac{\Gamma_{\text{cusp}}(\alpha)}{\beta(\alpha)} \simeq \frac{2C_F}{\beta_0} \ln \frac{\alpha_s(\mu_0)}{\alpha_s(\mu)}. \quad (83)$$

The hypergeometric function ${}_2F_1(a, b; c; z)$ has the series expansion

$${}_2F_1(a, b; c; z) = \sum_{n=0}^{\infty} \frac{\Gamma(a+n)\Gamma(b+n)\Gamma(c)}{\Gamma(a)\Gamma(b)\Gamma(c+n)} \frac{z^n}{n!}.$$

Starting from the tree-level result in the non-relativistic limit $\phi_B^+(\omega; \mu_0 = m) = \delta(\omega - m)$, we obtain for scales $\mu > m$ the relatively simple expression

$$m \phi_B^+(\omega; \mu) \Big|_{\text{tree}} = e^{V-2\gamma_E g} \frac{\Gamma(2-g)}{\Gamma(g)} \left(\frac{\omega_>}{m} \right)^g \frac{\omega_<}{\omega_>} {}_2F_1\left(1-g, 2-g; 2; \frac{\omega_<}{\omega_>}\right), \quad (84)$$

where now $\omega_< = \min(\omega, m)$, $\omega_> = \max(\omega, m)$, $g = g(\mu, m)$ and $V = V(\mu, m)$. Fixing the value of $\alpha_s(m)$ at the NR input scale, we may study how the shape of $\phi_B^+(\omega; \mu)$ is changed by evolution effects. In Figure 4 we have plotted (84) for $\alpha_s(m) = 1$ and three different values of $\eta = \alpha_s(\mu)/\alpha_s(m)$. As expected, the evolution drives the initial delta-function shape towards a flatter distribution. In the double-logarithmic plot on the right-hand side in Figure 4, we may read off the asymptotic behaviour of $\phi_B^+(\omega; \mu)$ for $\omega \rightarrow 0$ and $\omega \rightarrow \infty$. As argued on general grounds [23], the LCDA develops a linear behaviour for $\omega \rightarrow 0$, whereas for $\omega \rightarrow \infty$ it tends to fall off slower than $1/\omega$ at higher scales. This can also be seen by comparison with Figure 5, where we plot the evolution of another LCDA with initial condition $\phi_B^+(\omega; \mu_0 = m) = \omega/m^2 e^{-\omega/m}$.

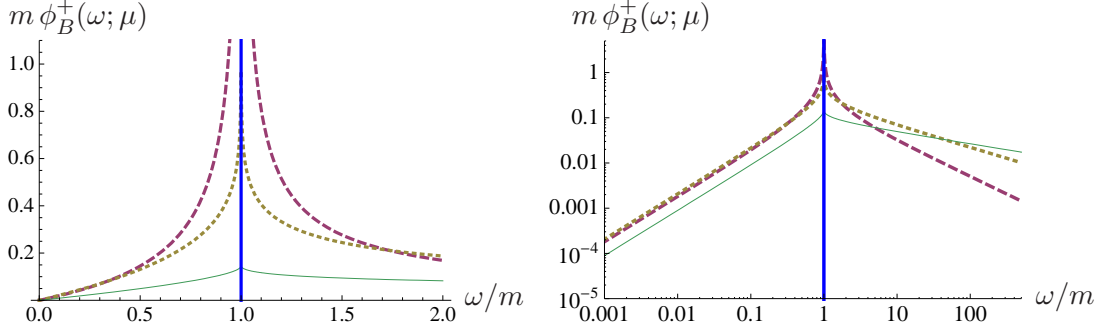


Figure 4: Evolution of the heavy meson LCDA $\phi_B^+(\omega; \mu)$ starting from the tree-level result $\phi_B^+(\omega; \mu_0 = m) = \delta(\omega - m)$, where we assumed $\alpha_s(m) = 1$ (thick solid line). The curves (dashed, dotted, thin solid line) correspond to $\eta = \alpha_s(\mu)/\alpha_s(m) = 1/2, 1/5, 1/10$, respectively.

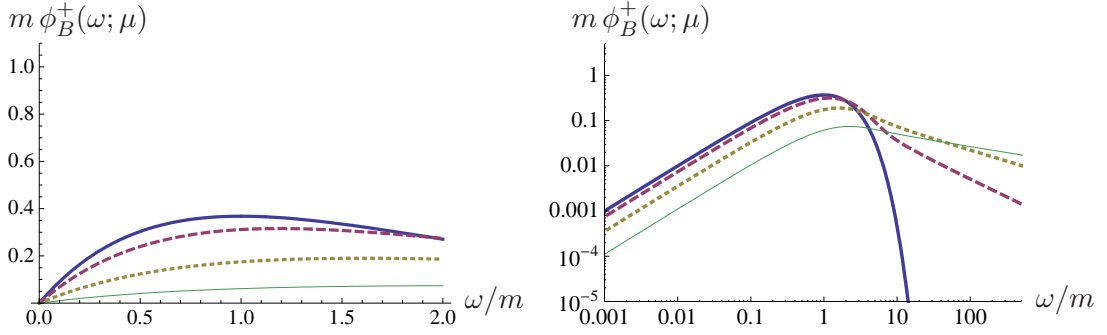


Figure 5: The same as Figure 4 with initial condition $\phi_B^+(\omega; \mu_0) = \omega/m^2 e^{-\omega/m}$ (thick solid line).

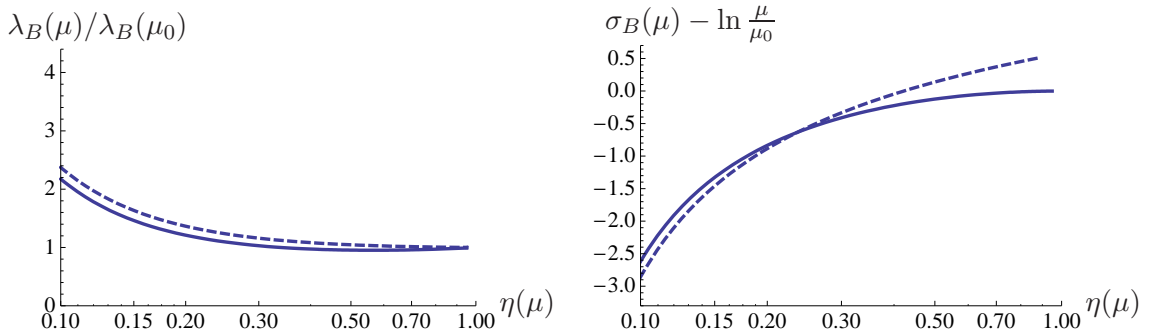


Figure 6: The moments $\lambda_B(\mu)/\lambda_B(\mu_0)$ and $\sigma_B(\mu) - \ln \mu/\mu_0$ as a function of the evolution parameter $\eta = \alpha_s(\mu)/\alpha_s(\mu_0)$. The solid line refers to the initial condition $\phi_B^+(\omega; \mu_0 = m) = \delta(\omega - m)$ and the dashed line to $\phi_B^+(\omega; \mu_0 = m) = \omega/m^2 e^{-\omega/m}$, where we assumed $\alpha_s(m) = 1$.

In Figure 6 we show the corresponding evolution of the phenomenologically relevant moments $\lambda_B(\mu)$ and $\sigma_B(\mu)$ defined in (51,53). From (81) we find the closed formulas

$$\frac{1}{\lambda_B(\mu)} = e^{V-2\gamma_E g} \frac{\Gamma(1-g)}{\Gamma(1+g)} \int_0^\infty \frac{d\omega}{\omega} \left(\frac{\omega}{\mu_0}\right)^g \phi_B^+(\omega; \mu_0), \quad (85)$$

$$\begin{aligned} \sigma_B(\mu) &= g(1-g) {}_4F_3(1, 1, 1-g, 2-g; 2, 2, 2; 1) \\ &\quad - \frac{g}{1-g} {}_3F_2(1-g, 1-g, 1-g; 2, 2-g; 1) \\ &\quad - \left(\int_0^\infty \frac{d\omega}{\omega} \left(\frac{\omega}{\mu_0}\right)^g \phi_B^+(\omega; \mu_0) \right)^{-1} \int_0^\infty \frac{d\omega}{\omega} \left(\frac{\omega}{\mu_0}\right)^g \ln \frac{\omega}{\mu} \phi_B^+(\omega; \mu_0). \end{aligned} \quad (86)$$

In general, the evolution of the moments λ_B and σ_B thus depends on the shape of the LCDA $\phi_B^+(\omega)$ [23]. For our examples, $\phi_B^+(\omega; \mu_0) = \delta(\omega - \mu_0)$, respectively $\phi_B^+(\omega; \mu_0) = \omega/\mu_0^2 e^{-\omega/\mu_0}$, the ω integration can be performed explicitly, leading to relatively simple analytic expressions. It is also possible to approximate the factors $(\omega/\mu_0)^g = 1 + g \ln(\omega/\mu_0) + \dots$. In this approximation, the evolution for the moment $\lambda_B(\mu)$ can be entirely determined in terms of $\lambda_B(\mu_0)$ and $\sigma_B(\mu_0)$, see also [24].

4.3 The LCDA $\phi_B^-(\omega)$

The evolution of the LCDA $\phi_B^-(\omega; \mu)$ is somewhat more involved, because of the possible mixing with the 3-particle LCDAs. In addition, for a non-vanishing light quark mass $m \neq 0$, we have seen in (59) that the LCDA $\phi_B^+(\omega; \mu)$ mixes into $\phi_B^-(\omega; \mu)$. In the following, we concentrate on possible applications in realistic B_q decays (where we can set $m = 0$), neglecting the contributions from 3-particle LCDAs which is left for future work. In this approximation, the solution of the evolution equation

$$\begin{aligned} \frac{d}{d \ln \mu} \phi_B^-(\omega; \mu) &= -\frac{\alpha_s C_F}{4\pi} \int_0^\infty d\omega' \gamma_-^{(1)}(\omega, \omega'; \mu) \phi_B^-(\omega'; \mu) + \mathcal{O}(\alpha_s^2) \\ &\quad + \begin{cases} \text{terms with } m \neq 0 \\ \text{contributions from 3-particle LCDAs} \end{cases} \end{aligned} \quad (87)$$

can be obtained in a similar way as for $\phi_B^+(\omega; \mu)$ [23, 35]. The details of the derivation can be found in Appendix D. As a result, the solution for $\phi_B^-(\omega; \mu)$ can be written as

$$\phi_B^-(\omega; \mu) \simeq e^{V-2\gamma_E g} \frac{\Gamma(1-g)}{\Gamma(g)} \int_0^\infty \frac{d\omega'}{\omega'} \phi_B^-(\omega'; \mu_0) \left(\frac{\omega_{>}}{\mu_0}\right)^g {}_2F_1\left(1-g, 1-g, 1, \frac{\omega_{<}}{\omega_{>}}\right). \quad (88)$$

In Figure 7 we illustrate the evolution of $\phi_B^-(\omega; \mu)$ for three different initial conditions at the scale $\mu_0 = m$:

- $\phi_B^-(\omega; \mu_0) = \delta(\omega - m)$,
- $\phi_B^-(\omega; \mu_0) = \theta(m - \omega)/m$,
- $\phi_B^-(\omega; \mu_0) = 1/m e^{-\omega/m}$.

The first example corresponds to the strict non-relativistic limit (where the neglect of the light quark mass in the evolution equation may be considered as inconsistent). The second and third example follow from the Wandzura-Wilczek relation (17) for the initial LCDAs $\phi_B^+(\omega; \mu_0)$ considered in the previous subsection. While the behaviour of $\phi_B^-(\omega; \mu)$ at small values of ω depends on the model for the initial distribution, the radiative tail for large values of ω is again universal. More precisely, the solution (88) of the (approximate) evolution equation suggests that $\phi_B^-(\omega; \mu)$ also falls off slower than $1/\omega$ at higher scales, while the slope of the LCDA at $\omega = 0$ tends to vanish under evolution, independent of the initial behaviour of the distribution amplitude.

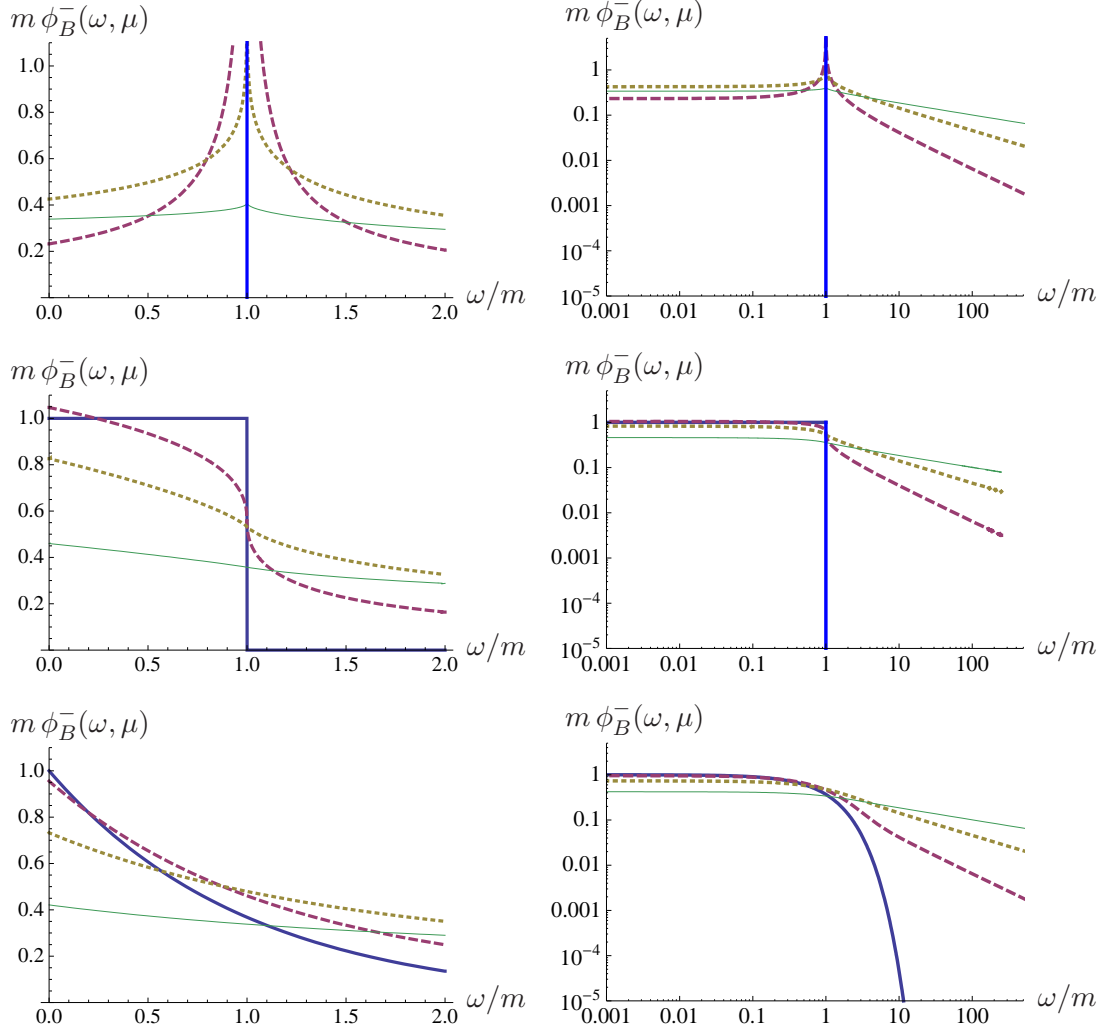


Figure 7: Evolution of the LCDA $\phi_B^-(\omega; \mu)$. Notations and conventions as in Figures 4,5. The initial conditions at the scale $\mu_0 = m$ are $\phi_B^-(\omega; \mu_0) = \delta(\omega - m)$ (upper row), $\phi_B^-(\omega; \mu_0) = \theta(m - \omega)/m$ (middle row) and $\phi_B^-(\omega; \mu_0) = 1/m e^{-\omega/m}$ (lower row).

5 Summary

Non-relativistic $q\bar{q}$ bound states have been used as a starting point to construct light-cone distribution amplitudes for light mesons in QCD and heavy mesons in HQET. At the non-relativistic scale, the leading 2-particle distribution amplitudes can be approximated by delta functions, fixing the light-cone momenta of the quarks according to their masses. After including radiative corrections from relativistic gluon exchange, the distribution amplitudes cover the whole physically allowed support region, $0 \leq u \leq 1$ for light mesons and $0 \leq \omega < \infty$ for heavy mesons. In this paper, explicit expressions for 2-particle distribution amplitudes of twist-2 and twist-3 for "light" mesons (with quark masses $m_1 \sim m_2$) have been calculated to first order in the strong coupling constant. In the same way, next-to-leading order expressions for the 2- and 3-particle distribution amplitudes have been derived for "heavy" mesons (where $m_1 \gg m_2$). We also studied the evolution of the 2-particle distribution amplitudes under change of renormalization scale.

Our results apply to the physical situation of a hard exclusive reaction, that involves bound states of heavy bottom or charm quarks, with large momentum transfer, for instance, $B_c \rightarrow \eta_c \ell \nu$ [27, 44–47], $e^+ e^- \rightarrow J/\psi \eta_c$ [48–51] or $\gamma^* \gamma \rightarrow \eta_c$ [52]. Moreover, from the divergence structure of our explicit next-to-leading order results, we could derive certain model-independent properties which also hold for bound states of relativistic quarks. In this way we used our calculation as a toy model to derive new results for the B meson distribution amplitude ϕ_B^- , as the cut-off dependence of positive moments, the anomalous dimension kernel and the solution of the evolution equation in the Wandzura-Wilczek approximation. The toy model also allowed us to address an issue that has been controversial in the literature, i.e. the question if the constraints from the equations of motion hold beyond tree level in the heavy meson case.

Acknowledgements

T.F. is supported by the German Ministry of Research (BMBF, contract No. 05HT6PSA). He also acknowledges financial support by the Cluster of Excellence "Origin and Structure of the Universe" during his stay at the TU Munich in fall 2007. The work of G.B. is supported by the DFG Sonderforschungsbereich/Transregio 9.

A One-loop corrections to $\phi_\pi(u)$

We briefly summarize our results for the individual diagrams in Figure 2 in the light meson case (in Feynman gauge). For simplicity we present the results for the leading-twist LCDA $\phi_\pi(u)$ and stick to the case $m_1 = m_2 = m$.

A.1 Vertex diagram

Starting from the NR limit $\phi_\pi(u) = \delta(u - 1/2)$ and performing the loop-integral in $D = 4 - 2\epsilon$ dimensions, one obtains for the first diagram in Figure 2 the distribution

$$I_a(u) \propto 4\Gamma(\epsilon) \left(\frac{\mu^2 e^{\gamma_E}}{m^2 (1-2u)^2} \right)^\epsilon \left(1 - \epsilon \frac{4u^2 - 4u - 1}{(1-2u)^2} \right) [u\theta(1-2u) + \bar{u}\theta(2u-1)]. \quad (89)$$

The integral contains an UV-divergence reflected by $\Gamma(\epsilon)$. The IR-divergence at $u = 1/2$ can be isolated with the help of a plus-distribution which we introduce via (29). With this we obtain

$$I_a(u) \propto 4 \left[\left(\frac{1}{\epsilon} + \ln \frac{\mu^2}{m^2 (1-2u)^2} - \frac{4u^2 - 4u - 1}{(1-2u)^2} \right) [u\theta(1-2u) + \bar{u}\theta(2u-1)] \right]_{++} + \left(\frac{3}{\epsilon} + 3 \ln \frac{\mu^2}{m^2} - 2 \right) \delta(u - 1/2). \quad (90)$$

Notice that the term with $\delta'(u - 1/2)$ vanishes due to the symmetry $u \leftrightarrow \bar{u}$ in the equal mass case (the “++”-distribution actually coincides with the usual “+”-distribution in this case). The local term determines a correction to the decay constant and does not contribute to $\phi_\pi(u)$.

A.2 Wilson-line diagrams

For the second diagram in Figure 2 we obtain

$$I_b(u) \propto 8\Gamma(\epsilon) \int_0^{1/2} dv \left(\frac{\mu^2 e^{\gamma_E}}{m^2(1-2v)^2} \right)^\epsilon \frac{v}{2v-1} [\delta(u-1/2) - \delta(u-v)]. \quad (91)$$

Convoluting with a regular test function, we get

$$\int_0^1 du f(u) I_b(u) \propto \int_0^1 du f(u) \left[\frac{8u\theta(1-2u)}{1-2u} \left(\frac{1}{\epsilon} + \ln \frac{\mu^2}{m^2(1-2u)^2} \right) \right]_+. \quad (92)$$

The other Wilson-line diagram in Figure 2 is obtained from I_b by symmetrization $u \rightarrow \bar{u}$.

B One-loop corrections to $\phi_B^\pm(\omega)$

In the following we present our results for the diagrams in Figure 2 in the heavy meson case (in Feynman gauge). We compute the first order corrections to the NR limit at the matching scale $\mu \sim m$ starting from $\phi_B^\pm(\omega_{\text{in}}) = \delta(\omega_{\text{in}} - m)$, and the general anomalous dimension kernels related to the renormalization of $\phi_B^+(\omega; \mu)$ and $\phi_B^-(\omega; \mu)$. The latter are extracted from the UV-divergent parts of the diagrams, where we consider arbitrary input functions $\phi_B^\pm(\omega_{\text{in}})$ and also keep track of the light quark mass $m \neq 0$. Notice, that a possible mixing of the 3-particle LCDAs into $\phi_B^-(\omega; \mu)$ is not considered. Some care has to be taken when performing the collinear limit (which amounts to setting the transverse momentum of the incoming light antiquark to zero).

B.1 Vertex diagram

The loop-integral in the first diagram of Figure 2 reads

$$\begin{aligned} \begin{pmatrix} I_a^+(\omega) \\ I_a^-(\omega) \end{pmatrix} &\propto - \int d\omega_{\text{in}} \int [dl] \frac{\delta(\omega - \omega_{\text{in}} + n_- l)}{[v \cdot l + i0] [l^2 + i0] [(l-k)^2 + i0]} \\ &\times \begin{pmatrix} n_- l - \omega_{\text{in}} + \frac{m^2}{\omega_{\text{in}}} \left(\frac{k_\perp \cdot l_\perp}{k_\perp^2} - 1 \right) & -m \frac{k_\perp \cdot l_\perp}{k_\perp^2} \\ -m \frac{k_\perp \cdot l_\perp}{k_\perp^2} & n_+ l - \frac{m^2}{\omega_{\text{in}}} + \omega_{\text{in}} \left(\frac{k_\perp \cdot l_\perp}{k_\perp^2} - 1 \right) \end{pmatrix} \begin{pmatrix} \phi_B^+(\omega_{\text{in}}) \\ \phi_B^-(\omega_{\text{in}}) \end{pmatrix} \end{aligned} \quad (93)$$

where $\omega_{\text{in}} = n_- k$ with k^μ being the momentum of the incoming spectator quark and $k^\mu - l^\mu$ is the spectator-quark momentum after the interaction with the gluon. We also performed the collinear limit $k_\perp \rightarrow 0$, which requires to keep terms of order $k_\perp \cdot l_\perp / k_\perp^2$.

Let us first consider the fixed-order corrections to the NR limit, where $\phi_B^\pm(\omega_{\text{in}}) = \delta(\omega_{\text{in}} - m)$. Then the loop integrals simplify according to

$$I_a^\pm(\omega) \propto \int [dl] \frac{2m - n_\mp l}{[v \cdot l + i0] [l^2 + i0] [l^2 - 2m v \cdot l + i0]} \delta(\omega - m + n_- l). \quad (94)$$

Performing the loop-integrals in $D = 4 - 2\epsilon$ dimensions, one is left with the distributions

$$\begin{aligned}
I_a^+(\omega) &\propto 2\omega \Gamma(1 + \epsilon) \left(\frac{\mu^2 e^{\gamma_E}}{(m - \omega)^2} \right)^\epsilon \left\{ \frac{2}{(m - \omega)^2} - \frac{\theta(m - \omega)}{m(m - \omega)} - \frac{\theta(\omega - m)}{\omega(\omega - m)} \right\} \\
&= 4\omega \left[\frac{\theta(2m - \omega)}{(m - \omega)^2} \right]_{++} + 4\omega \frac{\theta(\omega - 2m)}{(m - \omega)^2} - 2\omega \left[\frac{\theta(m - \omega)}{m(m - \omega)} + \frac{\theta(\omega - m)}{\omega(\omega - m)} \right]_+ \\
&\quad + 2 \left(\frac{1}{\epsilon} + \ln \frac{\mu^2}{m^2} - 4 \right) \delta(\omega - m), \tag{95}
\end{aligned}$$

$$\begin{aligned}
I_a^-(\omega) &\propto \frac{2(1 - \epsilon) \Gamma(\epsilon)}{m} \left(\frac{\mu^2 e^{\gamma_E}}{(m - \omega)^2} \right)^\epsilon \theta(m - \omega) \\
&\quad + 2m \Gamma(1 + \epsilon) \left(\frac{\mu^2 e^{\gamma_E}}{(m - \omega)^2} \right)^\epsilon \left\{ \frac{2}{(m - \omega)^2} - \frac{\theta(m - \omega)}{m(m - \omega)} - \frac{\theta(\omega - m)}{m(\omega - m)} \right\} \\
&= 2 \left(\frac{1}{\epsilon} + \ln \left[\frac{\mu^2}{(m - \omega)^2} \right] - 1 \right) \frac{\theta(m - \omega)}{m} + 4m \left[\frac{\theta(2m - \omega)}{(m - \omega)^2} \right]_{++} + 4m \frac{\theta(\omega - 2m)}{(m - \omega)^2} \\
&\quad - 2 \left[\frac{\theta(m - \omega)}{m - \omega} \right]_+ - 2\omega \left[\frac{\theta(\omega - m)}{\omega(\omega - m)} \right]_+ + 2 \left(\frac{1}{\epsilon} + \ln \frac{\mu^2}{m^2} - 4 \right) \delta(\omega - m). \tag{96}
\end{aligned}$$

The integration over ω determines the local vertex correction to be absorbed into the decay constant

$$\int_0^\infty d\omega I_a^\pm(\omega) \propto \left(\frac{3}{\epsilon} + 3 \ln \frac{\mu^2}{m^2} - 2 \right). \tag{97}$$

Focusing now on the UV-divergent contributions to the integration kernels in the general case, we find

$$I_a^+(\omega)|_{\text{div.}} \propto \mathcal{O}(\epsilon^0), \tag{98}$$

$$I_a^-(\omega)|_{\text{div.}} \propto \frac{2}{\epsilon} \int d\omega_{\text{in}} \left(\frac{\theta(\omega_{\text{in}} - \omega)}{\omega_{\text{in}}} \right) \phi_B^-(\omega_{\text{in}}) + \mathcal{O}(\epsilon^0). \tag{99}$$

Notice that only the kernel in I_a^- receives an UV-divergent piece, which can be traced back to the appearance of a factor $(n_+ l)$ in the numerator of (93). The fact that the kernel of I_a^+ is UV-finite is in line with the findings of [23].

B.2 Wilson-line coupling to heavy quark

In this case there is no mixing between ϕ_B^\pm and ϕ_B^\mp since the light-quark propagator is not involved

$$I_b^\pm(\omega) \propto - \int d\omega_{\text{in}} \int [dl] \frac{\delta(\omega - \omega_{\text{in}} + n_- l) - \delta(\omega - \omega_{\text{in}})}{(n_- l) [v \cdot l + i0] [l^2 + i0]} \phi_B^\pm(\omega_{\text{in}}). \tag{100}$$

Inserting the non-relativistic LCDAs and performing the $(n_+ l)$ and l_\perp integrations, one is left with the parameter integral ($k = -n_- l$)

$$I_b^\pm(\omega) \propto 2 \Gamma(\epsilon) \int_0^\infty dk \left(\frac{\mu^2 e^{\gamma_E}}{k^2} \right)^\epsilon \frac{\delta(\omega - m - k) - \delta(\omega - m)}{k}. \tag{101}$$

Notice that the remaining integral induces an additional UV-divergence, which has to be isolated by introducing appropriate plus-distributions. We find

$$I_b^\pm(\omega) \propto 2\omega \left[\left(\frac{1}{\epsilon} + \ln \left[\frac{\mu^2}{(\omega - m)^2} \right] \right) \frac{\theta(\omega - m)}{\omega(\omega - m)} \right]_+ - \left(\frac{1}{\epsilon^2} + \frac{1}{\epsilon} \ln \frac{\mu^2}{m^2} + \frac{1}{2} \ln^2 \frac{\mu^2}{m^2} + \frac{3\pi^2}{4} \right) \delta(\omega - m). \tag{102}$$

The UV-divergent contribution for I_b^+ corresponds to the result for the diagram (D1) in [23] (with $\omega' \equiv m$). The UV-divergence from $k \rightarrow \infty$ is a peculiarity of the heavy meson wave function. It is related to the cusp-anomalous dimension involving the heavy quark (characterized by a time-like vector v^μ) and the soft Wilson line (characterized by a light-like vector n_-^μ). The resulting $1/\epsilon^2$ terms are universal for ϕ_B^+ and ϕ_B^- ,

$$I_b^\pm(\omega)|_{\text{div.}} \propto -\left(\frac{1}{\epsilon^2} + \frac{1}{\epsilon} \ln \frac{\mu^2}{\omega^2}\right) \phi_B^\pm(\omega) + \frac{2}{\epsilon} \int d\omega_{\text{in}} \left[\frac{\theta(\omega - \omega_{\text{in}})}{\omega - \omega_{\text{in}}} \right] [\phi_B^\pm(\omega_{\text{in}}) - \phi_B^\pm(\omega)] + \mathcal{O}(\epsilon^0). \quad (103)$$

B.3 Wilson-line coupling to light quark

In this case the loop integrals mix ϕ_B^+ into ϕ_B^- (but not vice versa),

$$\begin{aligned} \begin{pmatrix} I_c^+(\omega) \\ I_c^-(\omega) \end{pmatrix} &\propto 2 \int d\omega_{\text{in}} \int [dl] \frac{\delta(\omega - \omega_{\text{in}} + n_-l) - \delta(\omega - \omega_{\text{in}})}{(n_-l) [(l-k)^2 + i0] [l^2 + i0]} \\ &\times \begin{pmatrix} \omega_{\text{in}} - n_-l & 0 \\ m \frac{k_\perp \cdot l_\perp}{k_\perp^2} & \omega_{\text{in}} \left(1 - \frac{k_\perp \cdot l_\perp}{k_\perp^2}\right) \end{pmatrix} \begin{pmatrix} \phi_B^+(\omega_{\text{in}}) \\ \phi_B^-(\omega_{\text{in}}) \end{pmatrix}. \end{aligned} \quad (104)$$

Inserting the non-relativistic LCDAs and performing the $(n+l)$ and l_\perp integrations, we find ($k = n-l$)

$$\begin{aligned} I_c^+(\omega) &\propto 2\Gamma(\epsilon) \int_0^m dk \frac{m-k}{m} \left(\frac{\mu^2 e^{\gamma_E}}{k^2}\right)^\epsilon \frac{\delta(k-m+\omega) - \delta(\omega-m)}{k} \\ &= 2\omega \left[\left(\frac{1}{\epsilon} + \ln \left[\frac{\mu^2}{(\omega-m)^2}\right]\right) \frac{\theta(m-\omega)}{m(m-\omega)} \right]_+ + \left(\frac{2}{\epsilon} + 2 \ln \frac{\mu^2}{m^2} + 4\right) \delta(\omega-m), \end{aligned} \quad (105)$$

$$\begin{aligned} I_c^-(\omega) &\propto 2\Gamma(\epsilon) \int_0^m dk \left(\frac{\mu^2 e^{\gamma_E}}{k^2}\right)^\epsilon \frac{\delta(k-m+\omega) - \delta(\omega-m)}{k} \\ &= 2 \left[\left(\frac{1}{\epsilon} + \ln \left[\frac{\mu^2}{(\omega-m)^2}\right]\right) \frac{\theta(m-\omega)}{m-\omega} \right]_+. \end{aligned} \quad (106)$$

The UV-divergent contributions to the integration kernels are identified as

$$I_c^+(\omega)|_{\text{div.}} \propto \frac{2}{\epsilon} \phi_B^+(\omega) + \frac{2}{\epsilon} \int d\omega_{\text{in}} \left[\frac{\omega \theta(\omega_{\text{in}} - \omega)}{\omega_{\text{in}} (\omega_{\text{in}} - \omega)} \right] [\phi_B^+(\omega_{\text{in}}) - \phi_B^+(\omega)] + \mathcal{O}(\epsilon^0), \quad (107)$$

$$\begin{aligned} I_c^-(\omega)|_{\text{div.}} &\propto \frac{2}{\epsilon} \phi_B^-(\omega) + \frac{2}{\epsilon} \int d\omega_{\text{in}} \left[\frac{\omega \theta(\omega_{\text{in}} - \omega)}{\omega_{\text{in}} (\omega_{\text{in}} - \omega)} \right] [\phi_B^-(\omega_{\text{in}}) - \phi_B^-(\omega)] \\ &\quad + \frac{2}{\epsilon} \int d\omega_{\text{in}} \left[\frac{m \theta(\omega_{\text{in}} - \omega)}{\omega_{\text{in}}^2} \right] [\phi_B^+(\omega_{\text{in}}) - \phi_B^+(\omega)] + \mathcal{O}(\epsilon^0). \end{aligned} \quad (108)$$

Our result for I_c^+ is in line with [23]. In particular, there are no additional UV-divergences related to cusp anomalous dimensions since the light-quark and the soft Wilson line are characterized by the same light-cone vector n_-^μ . For a non-vanishing light-quark mass, the result for I_c^- implies that the LCDA ϕ_B^+ mixes into ϕ_B^- under evolution. In the massless case, however, ϕ_B^+ and ϕ_B^- evolve independently (at least to leading logarithmic approximation).

C Equations of motion for heavy meson LCDAs

In this appendix we show that the eom-constraint (15) holds after including first order relativistic corrections to the NR limit. We first evaluate the right-hand side of (15) using our explicit results

for the 3-particle LCDAs from (67)

$$\begin{aligned}
& (D-2) \int_0^\omega d\eta \int_{\omega-\eta}^\infty \frac{d\xi}{\xi} \frac{\partial}{\partial \xi} [\Psi_A(\eta, \xi) - \Psi_V(\eta, \xi)] \\
&= \frac{\alpha_s C_F}{4\pi} \left\{ \left(\frac{1}{\varepsilon} + \ln \frac{\mu^2}{m^2} \right) m \delta(\omega - m) - \left[\frac{2\omega}{m} \left(\frac{1}{\varepsilon} + \ln \frac{\mu^2}{(m-\omega)^2} + 1 \right) + 2 \ln \frac{(m-\omega)^2}{m^2} \right] \theta(m-\omega) \right\}.
\end{aligned} \tag{109}$$

For the expressions on the left-hand side of (15), we obtain

$$\begin{aligned}
& \omega \phi_B^-(\omega) - m^{\text{bare}} \phi_B^+(\omega) \\
&= (m^{\text{OS}} - m^{\text{bare}}) \delta(\omega - m) + \frac{\alpha_s C_F}{4\pi} \left\{ \frac{2\omega}{m} \left(\frac{1}{\varepsilon} + \ln \frac{\mu^2}{(m-\omega)^2} - 1 \right) \theta(m-\omega) \right. \\
&\quad \left. + \left(\frac{2}{\varepsilon} + 2 \ln \frac{\mu^2}{(\omega-m)^2} - 2 \right) \theta(\omega-m) - \left(\frac{2}{\varepsilon} + 2 \ln \frac{\mu^2}{m^2} + 4 \right) m \delta(\omega-m) \right\}.
\end{aligned} \tag{110}$$

and

$$\begin{aligned}
& \frac{D-2}{2} \int_0^\omega d\eta [\phi_B^+(\eta) - \phi_B^-(\eta)] \\
&= -\frac{\alpha_s C_F}{4\pi} \left\{ \left[\frac{4\omega}{m} \left(\frac{1}{\varepsilon} + \ln \frac{\mu^2}{(m-\omega)^2} \right) + 2 \ln \frac{(m-\omega)^2}{m^2} \right] \theta(m-\omega) \right. \\
&\quad \left. + \left(\frac{2}{\varepsilon} + 2 \ln \frac{\mu^2}{(\omega-m)^2} - 2 \right) \theta(\omega-m) \right\}.
\end{aligned} \tag{111}$$

Noticing that

$$(m^{\text{OS}} - m^{\text{bare}}) = \frac{\alpha_s C_F}{4\pi} \left(\frac{3}{\varepsilon} + 3 \ln \frac{\mu^2}{m^2} + 4 \right) m + \mathcal{O}(\alpha_s^2),$$

we see that the equation of motion (15) is indeed fulfilled after including the α_s corrections.

D Solution of RGE for $\phi_B^-(\omega)$ in WW approximation

We derive the solution of the evolution equation (87) for the B -meson LCDA $\phi_B^-(\omega; \mu)$, ignoring the possible mixing with 3-particle LCDAs and neglecting the light quark mass m . We follow the analysis in [35], where a closed form for the LCDA $\phi_B^+(\omega; \mu)$ to LL approximation has been given. When the 3-particle LCDAs are neglected, $\phi_B^-(\omega; \mu)$ can be related to $\phi_B^+(\omega; \mu)$ by the Wandzura-Wilczek relation (17). This is also reflected in the leading-order result for the anomalous dimension kernels $\gamma_-^{(1)}(\omega, \omega'; \mu)$ from (60) and $\gamma_+^{(1)}(\omega, \omega'; \mu)$ from (48). Noticing that

$$-\omega \frac{d}{d\omega} \int_0^\omega \frac{d\omega'}{\eta} \left\{ \left(\Gamma_{\text{cusp}}^{(1)} \ln \frac{\mu}{\omega} - 2 \right) \delta(\omega - \omega') - \Gamma_{\text{cusp}}^{(1)} \frac{\theta(\omega' - \omega)}{\omega'} \right\} = \left(\Gamma_{\text{cusp}}^{(1)} \ln \frac{\mu}{\omega} - 2 \right) \delta(\omega - \omega), \tag{112}$$

and

$$\begin{aligned}
& \int_0^\omega d\eta f(\eta) \left\{ -\omega \frac{d}{d\omega} \int_0^\omega \frac{d\omega'}{\eta} \left[\frac{\theta(\omega - \omega')}{\omega - \omega'} \right]_+ \right\} = -\omega \frac{d}{d\omega} \int_0^1 \frac{dx}{x} \int_0^x \frac{dy}{1-y} f(\omega(1-y)) \\
&= \int_0^1 \frac{dx}{x} [f(\omega(1-x)) - f(\omega)] = \int_0^\omega d\eta f(\eta) \left[\frac{\theta(\omega - \eta)}{\omega - \eta} \right]_+,
\end{aligned} \tag{113}$$

and

$$\begin{aligned} \int_0^\infty d\eta f(\eta) \left\{ -\omega \frac{d}{d\omega} \int_0^\eta \frac{d\omega'}{\eta} \left[\frac{\omega \theta(\omega' - \omega)}{\omega'(\omega' - \omega)} \right]_+ \right\} &= \omega \frac{d}{d\omega} \int_0^\infty \frac{dx}{x(1+x)} \int_0^x \frac{dy}{1+y} f(\omega(1+y)) \\ &= \int_0^\infty \frac{dx}{x(1+x)} [f(\omega(1+x)) - f(\omega)] = \int_0^\infty d\eta f(\eta) \left[\frac{\omega \theta(\eta - \omega)}{\eta(\eta - \omega)} \right]_+, \end{aligned} \quad (114)$$

we find that the anomalous dimensions fulfill the relation

$$-\omega \frac{d}{d\omega} \int_0^\eta \frac{d\omega'}{\eta} \gamma_-^{(1)}(\omega, \omega'; \mu) = \gamma_+^{(1)}(\omega, \eta; \mu). \quad (115)$$

Therefore, the functions $\Phi_B^-(\omega; \mu) \equiv \omega d\phi_B^-(\omega; \mu)/d\omega$ and $\phi_B^+(\omega; \mu)$ obey the same evolution equation to LL approximation. Using an intermediate result from [35], we write the solution for $\Phi_B^-(\omega; \mu)$ as

$$\begin{aligned} \Phi_B^-(\omega; \mu) &= e^{V-2\gamma_E g} \left(\frac{\omega}{\mu_0} \right)^g \int_0^\infty \frac{d\omega'}{\omega'} \Phi_B^-(\omega'; \mu_0) \sum_{m=1}^\infty \frac{(-1)^{m+1} \Gamma(1+m-g)}{\Gamma(1-m+g)\Gamma(1+m)\Gamma(m)} \\ &\quad \times \left\{ \theta(\omega - \omega') \left(\frac{\omega}{\omega'} \right)^{-m} + \theta(\omega' - \omega) \left(\frac{\omega}{\omega'} \right)^{m-g} \right\} \\ &= e^{V-2\gamma_E g} \left(\frac{\omega}{\mu_0} \right)^g \int_0^\infty \frac{d\omega'}{\omega'} \phi_B^-(\omega'; \mu_0) \sum_{m=1}^\infty \frac{(-1)^m \Gamma(1+m-g)}{\Gamma(1-m+g)\Gamma(1+m)\Gamma(m)} \\ &\quad \times \left\{ m\theta(\omega - \omega') \left(\frac{\omega}{\omega'} \right)^{-m} + (g-m)\theta(\omega' - \omega) \left(\frac{\omega}{\omega'} \right)^{m-g} \right\}, \end{aligned} \quad (116)$$

with V and g from (82,83) and we assumed $0 < g < 1$. We finally perform the ω -integral to obtain $\phi_B^-(\omega; \mu)$ from $\Phi_B^-(\omega; \mu)$, and the summation over m which leads to hypergeometric functions with the result,

$$\begin{aligned} \phi_B^-(\omega; \mu) &= e^{V-2\gamma_E g} \frac{\Gamma(1-g)}{\Gamma(g)} \int_0^\infty \frac{d\omega'}{\omega'} \phi_B^-(\omega'; \mu_0) \left(\frac{\omega}{\mu_0} \right)^g \\ &\quad \times \left\{ \theta(\omega - \omega') \frac{\omega'}{\omega} {}_2F_1(1-g, 1-g, 1, \omega'/\omega) \right. \\ &\quad \left. + \theta(\omega' - \omega) \left(\frac{\omega}{\omega'} \right)^{-g} {}_2F_1(1-g, 1-g, 1, \omega/\omega') \right\}. \end{aligned} \quad (117)$$

References

- [1] V. M. Braun and I. E. Filyanov, Sov. J. Nucl. Phys. **52** (1990) 126.
- [2] P. Ball, JHEP **9901** (1999) 010 [hep-ph/9812375].
- [3] A. G. Grozin and M. Neubert, Phys. Rev. D **55** (1997) 272 [hep-ph/9607366].
- [4] M. Beneke and T. Feldmann, Nucl. Phys. B **592** (2001) 3 [hep-ph/0008255].
- [5] A. V. Efremov and A. V. Radyushkin, Phys. Lett. B **94**, 245 (1980); G. P. Lepage and S. J. Brodsky, Phys. Lett. B **87** (1979) 359; G. P. Lepage and S. J. Brodsky, Phys. Rev. D **22** (1980) 2157.
- [6] V. L. Chernyak and A. R. Zhitnitsky, Phys. Rept. **112** (1984) 173.
- [7] H. n. Li and H. L. Yu, Phys. Rev. D **53** (1996) 2480 [hep-ph/9411308]; H. n. Li and G. Sterman, Nucl. Phys. B **381** (1992) 129.

- [8] M. Beneke, G. Buchalla, M. Neubert and C. T. Sachrajda, Phys. Rev. Lett. **83** (1999) 1914 [hep-ph/9905312]; Nucl. Phys. B **591** (2000) 313. [hep-ph/0006124].
- [9] C. W. Bauer, S. Fleming, D. Pirjol and I. W. Stewart, Phys. Rev. D **63** (2001) 114020 [hep-ph/0011336]. C. W. Bauer and I. W. Stewart, Phys. Lett. B **516** (2001) 134 [hep-ph/0107001].
- [10] M. Beneke, A. P. Chapovsky, M. Diehl and T. Feldmann, Nucl. Phys. B **643** (2002) 431 [hep-ph/0206152]; M. Beneke and T. Feldmann, Phys. Lett. B **553** (2003) 267 [hep-ph/0211358].
- [11] I. I. Balitsky, V. M. Braun and A. V. Kolesnichenko, Nucl. Phys. B **312** (1989) 509.
- [12] V. M. Braun and I. E. Filyanov, Z. Phys. C **44** (1989) 157.
- [13] V. L. Chernyak and I. R. Zhitnitsky, Nucl. Phys. B **345** (1990) 137.
- [14] P. Colangelo and A. Khodjamirian, in “M. Shifman (ed.): *At the frontier of particle physics*, Vol. 3*, 1495” [hep-ph/0010175].
- [15] P. Kroll and M. Raulfs, Phys. Lett. B **387** (1996) 848 [hep-ph/9605264].
- [16] A. Schmedding and O. I. Yakovlev, Phys. Rev. D **62** (2000) 116002 [arXiv:hep-ph/9905392].
- [17] A. P. Bakulev, S. V. Mikhailov and N. G. Stefanis, Phys. Rev. D **67** (2003) 074012 [arXiv:hep-ph/0212250].
- [18] J. Gronberg *et al.* [CLEO Collaboration], Phys. Rev. D **57** (1998) 33 [hep-ex/9707031].
- [19] A. Khodjamirian, T. Mannel and M. Melcher, Phys. Rev. D **70** (2004) 094002 [hep-ph/0407226].
- [20] P. Ball, V. M. Braun and A. Lenz, JHEP **0605** (2006) 004 [hep-ph/0603063].
- [21] V. M. Braun *et al.*, Phys. Rev. D **74** (2006) 074501 [hep-lat/0606012]; A. Jüttner (UKQCD collab.), talk at *DA 06*, Durham (2006); L. Del Debbio, Few Body Syst. **36** (2005) 77;
- [22] M. Göckeler *et al.*, Nucl. Phys. Proc. Suppl. **161** (2006) 69 [hep-lat/0510089];
- [23] B. O. Lange and M. Neubert, Phys. Rev. Lett. **91** (2003) 102001 [hep-ph/0303082];
- [24] V. M. Braun, D. Y. Ivanov and G. P. Korchemsky, Phys. Rev. D **69** (2004) 034014 [hep-ph/0309330].
- [25] J. P. Ma and Z. G. Si, Phys. Lett. B **647** (2007) 419 [hep-ph/0608221].
- [26] V. V. Braguta, A. K. Likhoded and A. V. Luchinsky, Phys. Lett. B **646** (2007) 80 [hep-ph/0611021]; V. V. Braguta, Phys. Rev. D **75** (2007) 094016 [hep-ph/0701234]; arXiv:0709.3885 [hep-ph].
- [27] G. Bell, PhD thesis, LMU Munich 2006, arXiv:0705.3133 [hep-ph]; G. Bell and T. Feldmann, Nucl. Phys. Proc. Suppl. **164** (2007) 189 [hep-ph/0509347], G. Bell, Diploma thesis, RWTH Aachen 2003 (in German).
- [28] T. Feldmann and G. Bell, arXiv:0711.4014 [hep-ph].
- [29] N. Brambilla *et al.* [Quarkonium Working Group], CERN Yellow Report, CERN-2005-005 [hep-ph/0412158].
- [30] I. V. Anikin, A. E. Dorokhov and L. Tomio, Phys. Lett. B **475** (2000) 361 [arXiv:hep-ph/9909368].

- [31] H. Kawamura, J. Kodaira, C. F. Qiao and K. Tanaka, Phys. Lett. B **523** (2001) 111 [Erratum-ibid. B **536** (2002) 344] [hep-ph/0109181].
- [32] A. G. Grozin, Int. J. Mod. Phys. A **20** (2005) 7451 [hep-ph/0506226].
- [33] T. Huang, C. F. Qiao and X. G. Wu, Phys. Rev. D **73** (2006) 074004 [hep-ph/0507270].
- [34] V. Braun, *B-meson distribution amplitudes*, talk presented at Workshop on Light-Cone Distribution Amplitudes (DA'06), 28-30 September 2006 at the IPPP, Durham.
- [35] S. J. Lee and M. Neubert, Phys. Rev. D **72** (2005) 094028 [hep-ph/0509350].
- [36] E. Braaten and S. Fleming, Phys. Rev. D **52** (1995) 181 [hep-ph/9501296].
- [37] E. Bagan, P. Ball and V. M. Braun, Phys. Lett. B **417** (1998) 154 [hep-ph/9709243].
- [38] C. M. Arnesen, Z. Ligeti, I. Z. Rothstein and I. W. Stewart, hep-ph/0607001.
- [39] M. Neubert, Phys. Rept. **245** (1994) 259 [hep-ph/9306320].
- [40] F. De Fazio, T. Feldmann and T. Hurth, Nucl. Phys. B **733**, 1 (2006) [hep-ph/0504088], JHEP **0802** (2008) 031 [arXiv:0711.3999 [hep-ph]].
- [41] A. Khodjamirian, T. Mannel and N. Offen, Phys. Lett. B **620** (2005) 52 [hep-ph/0504091]; Phys. Rev. D **75** (2007) 054013 [hep-ph/0611193].
- [42] P. Ball and A. N. Talbot, JHEP **0506**, 063 (2005) [hep-ph/0502115].
- [43] V. Pilipp, hep-ph/0703180.
- [44] T. Huang and F. Zuo, Eur. Phys. J. C **51** (2007) 833 [hep-ph/0702147].
- [45] E. Hernandez, J. Nieves and J. M. Verde-Velasco, Phys. Rev. D **74** (2006) 074008 [hep-ph/0607150].
- [46] M. A. Ivanov, J. G. Körner and P. Santorelli, Phys. Rev. D **73** (2006) 054024 [hep-ph/0602050].
- [47] D. Ebert, R. N. Faustov and V. O. Galkin, Phys. Rev. D **68** (2003) 094020 [hep-ph/0306306].
- [48] H. M. Choi and C. R. Ji, Phys. Rev. D **76** (2007) 094010 [arXiv:0707.1173 [hep-ph]].
- [49] G. T. Bodwin, D. Kang and J. Lee, Phys. Rev. D **74** (2006) 114028 [hep-ph/0603185].
- [50] A. E. Bondar and V. L. Chernyak, Phys. Lett. B **612** (2005) 215 [hep-ph/0412335].
- [51] J. P. Ma and Z. G. Si, Phys. Rev. D **70** (2004) 074007 [arXiv:hep-ph/0405111].
- [52] T. Feldmann and P. Kroll, Phys. Lett. B **413** (1997) 410 [hep-ph/9709203].